Division of Engineering
BROWN UNIVERSITY
PROVIDENCE, R. I.

ENGINEERING MATERIALS RESEARCH LABORATORY



# MULTIAXIAL CREEP STUDIES OF 304 STAINLESS STEEL

W. N. FINDLEY and R. MARK

Oak Ridge National Laboratory
Operated by
Union Carbide Corporation
for the
U. S. Atomic Energy Commission
Subcontract No. 3599
Annual Report No. 2

UCC 3599/2
EMRL-58

November 1973

---

# CONTENTS

CONTENTS (continued)

# MULTIAXIAL CREEP STUDIES OF 304 STAINLESS STEEL

by

William Nichols Findley and Roger Mark*

## ABSTRACT

Experiments performed during the second year of Subcontract No. 3599 S1 for the period September 1, 1972, through August 31, 1973, are reported. Analysis and interpretation of the accumulated experimental results were made in the month of September 1973 and are included in this report.

Tests in combined tension and torsion, pure tension and pure torsion, see Table I, were conducted at elevated temperatures (about 1100°F) for times ranging from 601.1 hours to 1009.25 hours. Additional tests were performed after the long-time creep tests as described in this report. Attempts to detect circumferential strains were made. Tests for which the initial conditions were similar to those reported in [1]** show strain rate vectors which are consistent with a Mises equivalent for a creep surface.

The best fit of the long-time creep and recovery data to the equation

$$\varepsilon_{ij} = \varepsilon_{ij}^{o} + \varepsilon_{ij}^{+} t^{n} \qquad (1)^{***}$$

was obtained by means of a least squares method. Equation (1) was found to describe the data satisfactorily when the strains were small (less than 1 per cent). By using (1) and a modified superposition principle for metals an

---

* Professor of Engineering and Research Assistant, respectively, Division of Engineering, Brown University, Providence, Rhode Island.

** Numbers in brackets denote references listed at the end of this report.

*** Numbers in parentheses denote equations.

expression was obtained describing a creep test involving stress reversals. A formulation involving a strain hardening assumption was made for the same test, and a comparison of the fit of the experimental data with the two expressions is given in this report.

## INTRODUCTION

This report reviews the work performed on Subcontract No. 3599 S1 during the second twelve months, from September 1, 1972, through August 31, 1973. For the sake of completeness, work done during September 1973 on the representation of the observed creep behavior by (1) and on the interpretation and prediction of creep under reversals in torsional stress is also included in this report. During this period the following people were employed on this work part-time: W. N. Findley, Professor of Engineering; R. Mark, Research Assistant; R. M. Reed, Technical Assistant; and R. Dean, Machinist.

The need for the work covered by this subcontract resulted from the fact that the higher temperatures and long life expected for liquid-metal fast-breeder reactors combine to cause creep behavior of the material to become a limiting feature in the design for efficient and safe production of nuclear energy. One of the principal structural materials for critical parts is type 304 stainless steel. However, information available on the creep behavior of this material is limited largely to uniaxial tension stresses. Since the design of many of the most critical parts involves biaxial stress states, varying stress and stress gradients, much more information is needed for design of these critical components for long-time service.

## MATERIAL

The material being investigated is type 304 stainless steel, ORNL reference heat number 9T2796, supplied by Oak Ridge National Laboratory. Four 12-foot bars numbered 16, 17, 18, and 22, 1.92 to 1.93 inches in diameter were supplied.

## EXPERIMENTAL RESULTS AND DISCUSSION

### Constant Load Creep Tests

During the reporting period six long-time creep tests under combined tension-torsion, pure tension and pure torsion were performed at a constant nominal temperature of 1100°F (see Table I) using six different specimens from the same bar (No. 16). Creep data from these six experiments and from the three tests given in [1] are presented in Fig. 1 through 9. The total axial strain $\epsilon_{11}$ and the total shear strain $\epsilon_{12}$ are plotted versus time $t$ to two different time scales, one showing the early part of the test (0 to 10 hours) and the other showing the entire constant stress test.

#### Long-time Creep at 15 Ksi Effective Mises Stress

The strains in Test No. 4 ($\sigma^{\text{Mises}}_{\text{effective}}$ = 18,175 psi) were much larger than expected due to an error in loading. These high shear strains caused an interference between the extensometer and parts of the testing machine. Readjustment of the components at 724.25 hours produced a slight change in the creep behavior (see Fig. 4). Because of the error in rebalancing the testing apparatus when the test was modified to accommodate stress reversals, the stress applied to the specimen was $\tau$ = 10,493 psi, 1,833 psi higher than the initially programmed torsional stress. Since a stress of 1,833 psi (undetected at the time) was present when the zero reading was taken at the test temperature, the observed values of the total shear strains in Test No. 4, shown in Fig. 4 and 4b, are less than what they should be by a constant amount. The difference may be approximated by the elastic shear strain due to a 1,833 psi stress in torsion at the test temperature, if the creep strains during the 25-hour preheating period for a shearing stress of 1,833 psi are assumed to be negligibly small. However, the creep rates and the trend in the creep strains shown in Fig. 4 and 4b are valid.

Test No. 5 was planned as a repeat of Test No. 1 [1] ($\sigma$ = 10,628 psi, $\tau$ = 6,111 psi, $\sigma^{\text{Mises}}_{\text{effective}}$ = 15 ksi). All tests following Test No. 1 (especially No. 2) showed larger strains than Test No. 1. Initial strains for Test No. 5 were about twice those of Test No. 1 and larger creep rates were observed, as shown in Table II.

After about 800 hours of testing the stress in the specimen was accidentally reduced for about 26 hours, because the dead weights which stressed the specimen came in contact with the mechanical jack used to apply and remove the load. After the jack was lowered the specimen continued to creep at the previous rate. A slight, almost unnoticeable change in the strains shown in Fig. 5 can be seen during this time period.

Large creep strains were also observed in Test No. 6 in which the specimen was subjected to a 15 ksi stress in pure tension. At about 500 hr. the creep rate began to increase rapidly (tertiary creep). Temperature observations during this period were normal. The unexpected large creep caused the loading weights to rest on the loading jack unintentionally for a short time. When these weights were freed the strain increased considerably, breaking the control thermocouple located inside the specimen and shutting off the heat. After removal of the specimen it was found that a cracked fitting had allowed cooling water to seep onto the top end heater leaving calcium deposits. Also, the lower half of the specimen contained many transverse cracks. Both end heaters were burned out, but the lamp was still functional. It appears that overheating contributed to the cracking. If so, the overheat was of only short duration because temperature readings were no more than 1125°F at any point up to 571.9 hr. At 601.1 hr. it was observed that the average temperature was still normal but the top of the specimen was cool and the bottom temperature was at about 1230°F. After 601.1 hr. the average temperature

decreased rapidly. No mechanism by which the lower heater could have produced overheating has been uncovered, however.

Test No. 7 was performed using the same ratio of $\sigma/\tau$ as Test No. 2 [1], except that an effective Mises stress of 15 ksi was used instead of 15,170 psi. The test was conducted at stresses of 13,819 psi in tension and 3,369 psi in torsion for 1,006.9 hr. The specimens for this test (and for Tests 8 and 9 at 10 ksi effective stress) were prepared by finishing the bore by honing and finishing the O.D. by grinding under coolant after heat treatment, see page 7, Machining.

Long-time Creep at 10 Ksi Effective Mises Stress

Tests 8 and 9 were performed in pure torsion and pure tension, respectively, at an effective Mises equivalent stress of 10 ksi. By conducting experiments at a lower stress level, some problems associated with large creep strains, such as those described above, may be avoided. Also the lower stresses are considered to be more representative of realistic design stresses. After 1,000 hours the maximum strains were 0.1691 per cent and 0.1503 per cent for Tests 8 and 9 respectively.

## Temperatures for the Long-time Creep Tests

The temperature of all thermocouples was recorded at regular time intervals throughout a test. After completion of an experiment the average of the temperatures of all thermocouples at each time of observation was computed. Then an average of these results was determined. This overall average is given in Table I. It should be noted that the temperature was determined from a strip chart recorder in conjunction with a L & N potentiometer for Tests 1 and 2, whereas a Doric digital temperature indicator was employed in subsequent tests. The digital instrument has a sensitivity of 1/10°F compared to a sensitivity of 1°F for the recorder and potentiometer.

## Fit of Long-time Creep Data to a Power Function

An analysis of the test data was made to determine how well the long-term creep data in Tests 1 through 9 could be described by (1). The results are shown in Fig. 1 to 9 and the values of the constants in (1) are given in Table III. The intrinsic nature of (1) is such that it will describe primary-type creep if $n$ is less than 1.

The curves shown in Fig. 1 to 9 were obtained by employing a least squares fit of the creep data. The time interval from 0 hours to t hours for which the creep strains were analyzed was reduced automatically in the analysis until the agreement between the "reduced" data and (1) was within a specified relative error, i.e., the ratio of the rms calculated from the data to the maximum strain in the resulting time period. The value of this ratio was selected as 0.012 or 1.2 per cent relative error.

## Creep Surface and the Effective Strain Rate Vector

The possibility that the direction of the strain rate vector and the magnitude of the effective creep rate (the time derivative of the effective strain) can be used to define a creep surface at a particular instant of time has been explored in [1] and [2]. By plotting the vectors for Tests 1 through 9 in stress space, see Fig. 10*, it was observed that the directions of the vectors at 120 hr. are nearly coincident with the normal to the Mises ellipse, but the strain rates are variable. See page 7 for a discussion of causes of the variation. The directions of most of the vectors lie slightly to the left of the Mises normals suggesting a creep surface (ellipse) whose $\tau$ axis is somewhat shorter than the

---

*The strain rate vector for Test No. 11, a test conducted at the time this report is being prepared, has been included for further clarification of the creep surface.

Mises ellipse. In addition the vectors for Tests 11, 3, 5, 7 and 6 show decreasing magnitudes as the ellipse is traversed from pure torsion (left) to pure tension (right). See Table II* and Fig. 10. This also supports the hypothesis that the $\tau$ axis of the creep surface (ellipse) is somewhat shorter than the Mises ellipse.

## Comparison of Related Experiments

The stress state in Test No. 1 ($\sigma$ = 10,628 psi and $\tau$ = 6111 psi) was repeated in Test No. 5. The creep during the 1000 hr. under constant load is shown in Fig. 5 for both $\varepsilon_{11}$ and $\varepsilon_{12}$. These results show about twice the initial strains in Test 5 compared to Test 1 and larger creep rates, as shown in Table II. See the section on Possible Causes of the Variation in Creep Rate, page 7, for further discussions.

Test No. 7 was similar to Test No. 2 in that they were both performed at the same stress ratio $\sigma/\tau$. The effective Mises stress in Test 7 was 15 ksi while it was 15,170 psi in Test 2. Results for Test 7 are shown in Fig. 7. Comparison of these results with those for Test 2 show that the creep rates in both tension and torsion were significantly less in Test No. 7 than in Test No. 2. Initial and one-hour strain readings were larger in tension and smaller in torsion for Test No. 7 than Test No. 2, see Table II. The direction of the strain rate vector for Test No. 7 (shown in Fig. 10) moved somewhat farther away from the Mises equivalent than Test No. 2. The creep rate at 120 hr. in Test No. 7 was about 1/10 that in Test No. 2. The only known differences in initial conditions between Test No. 7 and Test No. 2 are the following: (a) the effective stress was slightly lower in Test No. 7 than in Test No. 2, and (b) the specimen in Test No. 2 was finished by machining, whereas the specimen in Test No. 7 was finished by honing the bore and grinding the outside diameter.

*The magnitude of the effective strain rate vector can be evaluated by

$$\bar{\dot{\varepsilon}} = [(2/3)\dot{\varepsilon}_{ij}\dot{\varepsilon}_{ij}]^{1/2} \quad .$$

## Possible Causes of Variations in Creep Rate

Because of the variations in creep rate observed, especially between Tests 2 and 7 performed at about the same effective stress, an effort was made to find and minimize the cause. The following possibilities were investigated. None of them appear to be sufficient to explain the large creep rate observed in Test 2.

### Prior Plastic Strain

To familiarize test operators with technique before the first actual test, the specimen for Test 1 was subjected to a mock test at room temperature several times during which the load to be employed in the creep test at 1100°F was applied for short periods. Some plastic strain resulted from each load application, as shown in Table IV. These plastic strains may have lowered the plastic and creep strains in the subsequent creep test. However, it did not account for the difference between the creep rate of Tests 1 and 2 since the creep rate in Test 1 is reasonably consistent with that of other creep tests except for Test 2. The prior plastic strain in Test No. 1 apparently lowered the plastic strain occurring on loading at temperature during the creep test. By substracting the $\varepsilon_{11}^{o}$ and $\varepsilon_{12}^{o}$ terms in (1) for Test 1 from the corresponding terms for Test 5 the difference in plastic strain is found. Test 5 had a greater plastic strain than Test 1: 0.4173 per cent and 0.5371 per cent in tension and torsion, respectively.

### Machining

Work hardening during final machining is another possible cause of variation in plastic strain and creep rate. All specimens tested at an effective stress of 15 ksi, except Specimen No. 4 (Test 7) tested as a repeat of Test 2, were finish machined after heat treatment. This was done to eliminate the possible effects of warping and oxidation resulting from heat treatment. The machining

seems unlikely to account for the difference between Tests 1 and 2 since the two specimens were prepared at the same time with closely the same technique.

Details of machining of Specimens 1 and 2 are as follows. Specimen No. 1 was bored to an I.D. of about 0.840 in. using an HSS tool. Since this did not cut well, an all-purpose carbide tool (A83) was used to finish machine the bore. The outside of Specimen No. 1 was rough machined with a Stellite tool and finished with A83 carbide. The depth of cut varied between 0.003 and 0.006 in. The latter was found necessary in order to produce a good finish. The feed used was 0.002 in. The tools were sharpened for each specimen. The machining of Specimen No. 2 was done with A83 carbide. The final cuts used the same speed, feed and depth of cut as Specimen No. 1.

To determine whether the work hardening nature of 304 stainless would permit finishing by honing, thus perhaps reducing the amount of work hardening during finish machining, Specimen No. 4-304-16 was finished by honing the bore and grinding the outside of the test section to finish dimensions. The grinding was done on a cylindrical grinder. Ample coolant was used in both operations and care was taken to insure that cutting not burnishing occurred. The results were very satisfactory. Also, the cost was reduced and uniform diameters were produced, which was not possible with single point machining because of tool wear.

Since there was no evidence of recrystallization at the surface of Specimens 2 and 12, as would be expected from work hardening, and since some warping might result from heat treatment after finish machining, it was decided to finish subsequent specimens (for tests at 10 ksi) by honing the bore and grinding the outside.

Specimen No. 4 (Test 7), finished by honing, was tested at about the same stress as Test 2. The results showed much less creep than Test 2 and the results were more consistent with other test results.

Heat Treatment

The heat treating technique was reexamined to try to insure a homogeneous set of specimens. A new copper cooling plug was prepared to minimize possible warping during cooling from 2000°F by providing more uniform cooling. This plug was made to fit closer to the bore of the specimen and was provided with narrow lands so that only small areas of contact with the specimen were possible. Also a pad of steel wool was inserted at the top of the furnace to trap any oxygen entering at that point. An old specimen was heat treated by this method and checked for warping. No warping was observed.

Numerous particles were observed in samples which had been heat treated and polished. After etching with stainless steel etch (composed of $HNO_3$ - 10 ml; acetic - 10 ml; HCl - 15 ml; glycerol - 5 ml) many of these developed large holes. Accordingly, several tests were made to try to identify these features.

A set of small specimens (segments of a disc) were prepared 0.060 in. thick and machined in the same manner as the specimens. These were taken from the same region of the bar stock as the test section of tubular specimens. These small specimens were then heat treated at the same time at 2000°F and cooled in the same manner as the tubular specimens. However, each was subjected to a different time at temperature. The shortest time was 30 min. and others were removed from the oven at 15 min. intervals. No change in the microstructure was observed.

Micrographs transverse to the axis showed all particles to be round. Parallel to the axis there are round particles, segmented particles and long particles. The first of these were presumed to be chromium carbide, the second larger particles of the same which had been broken up during rolling, and last magnesium sulfide.

The large spots after etching were thought to be chromium carbide particles with a chrome-depleted zone around them. To check this an electron beam

probe was used to make a chromium trace across some of these particles. No depleted zone was found, but the particles were high in chrome. The elongated particles were manganese sulfide.

Microhardness tests over the large spots shown in micrographs after etching indicated softer values (i.e., holes). Similar tests on particles on unetched samples showed increased hardness compared to regions with no particles.

Hardness

Rockwell hardness readings were taken on the as-received material, the enlarged ends of several specimens, the test section of Specimens 2 and 12, after these specimens were sectioned, and on heat-treated small specimens (sections of a disc or "chips"). These values are shown in Table V. No significant variation was found between similar locations between specimens. There appeared to be an increase in hardness after creep testing compared to the heat treated chips: A38 to A45.

Grain Size

Grain size of specimens was examined as a possible explanation for the different creep rates between specimens. Pieces cut from the shoulder of Specimens No. 1, 2 and 5 were examined first. These showed no significant difference in grain size. However, small particles thought to be chrome carbides and elongated particles thought to be sulfides were found. An attempt was made to polish and etch the outside of the test section as a possible means for checking grain size before testing. This method is not promising although some grain boundaries were visible.

Subsequently, Specimens 2 and 12 were sectioned and examined on planes transverse and parallel to the specimen axis. From polished and etched samples the number of grain boundaries across the 0.060 in. wall was determined to be

approximately 12.6 for Specimen No. 2 and 12 for Specimen No. 12, based on an average of several counts excluding twin boundaries. (The number was 20 for both specimens if twins were included.)

This grain size relative to the wall thickness is somewhat near the region dividing the material behavior from that of a polycrystalline material on one hand to that of a single crystal on the other hand. The critical grain size and nature of the transition from polycrystalline to single crystalline behavior appears not to be known for 304 stainless. Such information would be useful.

Nonlinearity

If the nonlinearity of 304 stainless is as strong as has been reported, small variation in stress could account for large changes in creep rate. Test 2 had stresses somewhat greater than the 15 ksi Mises effective stress used for Tests 1, 5, 6 and 7. Hence a greater creep rate would be expected. However, the much greater effective stress in Test 4 than Test 2 did not produce nearly as large a creep rate as Test 2. An analysis of the possible effect of nonlinearity was started but not completed because of insufficient data.

Temperature Variation

The observed average temperature varies somewhat from test to test as shown in Table I. How much of the observed variation is real is uncertain since the thermocouple wire has a variability resulting in a temperature uncertainty of ± 3/8 per cent at 1100°F, a limit of error of ± 4.1°F. Since the creep rate is very sensitive to temperature, as will be discussed later, some of the variation among test results may be due to temperature variations.

Stressing Error

An error in stressing in Test No. 2 possibly may be the cause of the large creep rate. All sources of such errors which can be checked have been checked, and

no error has been found. However, the stress for Test 4 was not on the 15 ksi Mises ellipse. Also the stresses for Tests 2 and 3 were slightly off the 15 ksi Mises ellipse because the early results suggested a slightly different creep surface than the Mises, see [1].

## Grain Size

Micrographs of etched samples from several specimens were compared with ASTM grain size charts. The results indicate a grain size of ASTM #3.

## Hardness

As shown in Table V the as-received hardness of bar No. 16 was Rockwell C35. After heat treating at 2000°F followed by rapid cooling the hardness was Rockwell A37.

## Supplementary Tests

After the long-time creep tests, several additional experiments were performed in Tests 4, 5, 7, 8 and 9. No subsequent testing was done in Test 6 because it was terminated early due to reasons given in the section on Long-time Creep at 15 Ksi Effective Mises Stress, page 2. Only recovery after 1000 hours of creep was observed in Test No. 7 (see Fig. 7a and 7b). The loading programs employed in the supplementary tests are shown in Tables VI, VII, VIII and IX. The experimental data are given in Fig. 4a, 4b, 4c, 5a, 5b, 7a, 7b, 8a, 8b and 9a.

### Recovery

Periods of recovery after creep were observed in Tests 5A, 5C, 5E and 5G in Test No. 5 (see Table VII); Test 7A in Test No. 7 after 1000 hours of creep; and Tests 9A and 9C in Test No. 9 (see Table IX). The recovery strains in these tests were fitted by an equation similar to (1) in order to determine the time-independent strain and rates of recovery. It has been previously reported in [1] that a small time-dependent recovery occurred after long-time creep. This type

of behavior was also observed in the additional tests so far completed on 304 stainless steel (see Fig. 5a, 5b, 7a, 7b and 9a, where the recovery curves and data are shown, and Table X). In Table X the constant (time-independent) coefficients $\epsilon_{ij}^{o}$ were obtained by subtracting the strain reading taken before unloading from the time-independent term evaluated from the least squares fit of the recovery data. Upon unloading to zero load it seems reasonable to expect that the time-independent strain would be elastic (if not affected by a Bauschinger effect). Under this assumption it is possible to determine Young's modulus E and/or the shear modulus G by dividing the time-independent strains given in Table X by the stress applied during the period of creep preceding recovery. This procedure has been followed through in Table X where the elastic moduli are given along with the corresponding temperatures. These results are quite consistent among themselves and reasonably consistent with moduli reported elsewhere.

Changes in Stress State and Temperature

Subsequent to 1009.25 hr. of creep in Test No. 4 the shearing stress was changed abruptly several times as detailed in Table VI. Other experiments include tension creep tests in combination with a small torque, an abrupt increase in temperature to 1170°F, an abrupt decrease in temperature to 1110°F, recovery at a small shear stress followed by reloading and another recovery with a small torque (see Fig. 4a and 4b).

In Fig. 4c are shown the shear strain vs. time for the two reverse loading cycles, Test No. 4A, 4B, 4C, 4D, described in Table VI. The temperature shown is the average temperature during this portion of the experiment. Tests 4A through 4D exhibited similar creep responses. The time-independent strain (elastic plus plastic) was less in the second negative loading than the first in spite of the stress change being somewhat greater, the time-independent

strain on positive reloading was less in the second than the first, and both positive reloading strains were greater than the negative loading strains. The negative loading creep curves were essentially identical except for a displacement of origins, and both showed continuously decreasing creep rates. The positive reloading creep curves seemed to have a short-time transition followed by an approach to the same constant rate of about 0.002 per cent/hr. compared to a creep rate of about 0.0017 per cent/hr. preceding the first negative loading.

Subsequent to the 1000 hr. at constant load in Test 5 recovery was observed and a program of other loadings was performed. This program was similar to that following Test No. 1 [1] but in opposite sequence. The program is outlined in Table VII together with representative strains.

After two periods of creep and two periods of recovery, preliminary investigations into the effect of minor temperature variations on creep rate were made in Tests 9D through 9G of Test 9. The strain rates associated with each temperature are shown in Table XI. Increasing the temperature by 24°F increased the creep rate about three times, while decreasing the temperature 32°F reduced the creep rate by a factor of 1/4. This information reveals how critical it is to maintain the test temperature at a constant value with time as well as along the specimen gage length. It may also explain some of the discrepancies found in the trend in the test data (e.g., see section on the Mises creep surface, page 5).

Creep under Stress Reversals

Subsequent to 1007 hours of creep at 5773 psi in torsion (effective Mises stress of 10 ksi), the stress was reversed several times in Test No. 8. Both positive and negative stresses were of the same magnitude. The creep behavior observed in Test 8 was similar to that seen in Test No. 4 except that in Test 4 the instantaneous response for "positive reloadings" was greater than that for

"negative loadings," in contrast to Test No. 8 where the instantaneous response for "negative loadings" was greater than that for "positive reloadings." An explanation for this difference is that the negative stresses (whose magnitudes were less than the positive reloading stresses) in Test No. 4 did not advance beyond the yield surface as far as the positive stresses, resulting in less plastic strains. Since the stresses for positive and negative loadings in Test No. 8 were equal in magnitude, more equal plastic strains resulted.

The experimental data for the stress reversals in Test No. 8 are shown in Fig. 8a. The curved line shown in the same figure was obtained by using a modified superposition principle and by assuming that the magnitude of the plastic strains changes with the number of cycles. The modified superposition principle [3] was developed for nonlinear materials. As used for plastics, this principle predicts much greater recovery upon the removal of the creep stress than found for metals. However, for metals the principle may be restated as follows: At a change in stress at time $t_1$, it may be considered that the strain is the sum of (a) the strain that would have occurred had the stress not been changed, plus (b) the strain due to the application of an equal but opposite stress at time $t_1$ (i.e., recovery), plus (c) the strain that would have occurred had the current stress been applied at time $t_1$.

This interpretation of the modified superposition principle may not work in general. For example, if at time $t_1$ the load is considered to be removed and then instantly reapplied, the above predicts an abrupt change in creep rate after $t_1$, assuming that the character of the time-dependent strains resulting from the application of an opposite stress in part (b) (recovery) is different from that in parts (a) and (c). This is not in accordance with prior observations on the creep of 1100AL and Cr-Mo-V steel [4,5]. Nevertheless, the above concept

has been employed in the following analysis of the reverse loading creep tests in Test 8.

The plastic strains in part (c) depend on the prior stress history of the specimen. The instantaneous response (comprised of elastic and plastic components) was determined by the following scheme: (a) obtain a least-squares fit of the data for phase II to the equation $\varepsilon_{12} = A + Bt^m$, (b) evaluate the final theoretical value for strain in phase I (at $t = t_1$) by means of (1), (c) subtract the constant $\varepsilon_{12}^{o} + \varepsilon_{12}^{+} t_1^{n}$ determined from (b) from the constant $A$ determined in (a). The result is the instantaneous response for phase II. A similar procedure was used to determine the instantaneous responses for the other phases. Assuming that the elastic component for the instantaneous response for phases II through VI was twice that for phase I and that the elastic strain $\varepsilon_{12}^{e}$ for phase I was 0.0347 per cent* (for a 5773 psi shear stress), the following plastic strains for each phase were computed:

| Phase I | Phase II | Phase III | Phase IV | Phase V | Phase VI |
|---|---|---|---|---|---|
| 0.0378% | 0.0496% | 0.0379% | 0.0437% | 0.0363% | 0.0370% |
| $\varepsilon_I^p$ | $\varepsilon_{II}^p$ | $\varepsilon_{III}^p$ | $\varepsilon_{IV}^p$ | $\varepsilon_V^p$ | $\varepsilon_{VI}^p$ |

The trend in the plastic strains with respect to the number of reversals suggests kinematic hardening in the yield surface (e.g., a larger plastic strain in phase II than in phase I) in conjunction with a change in size of the yield surface, indicated by decreasing plastic strains with increasing reversals (see phases II, IV, VI). Note, however, that the plastic strain on each reloading,

*This value for the elastic strain was obtained by assuming a shear modulus of $8.32 \times 10^6$ psi at 1110.6°F (determined by interpolation of the values of $E$ and $\nu$ given in Table 9.1 of [6].

phases III and V, were essentially the same as on the first loading.

Most of the recovery data at $\sigma_{eff}^{Mises}$=15 ksi and 10 ksi in this report and in [1] show a small time dependence. Since the recovery following torsion at an effective stress of 10 ksi is unknown at present, it has been assumed in the analysis that the recovery in part (b) was constant. Thus, the equations for each phase are as follows:

Phase I

$$\varepsilon_{12} = (\varepsilon_I^{\,p} + \varepsilon^e) + \varepsilon_{12}^{\,+} t^n \quad , \qquad t < t_1 \ , \ (2)$$

Phase II

$$\varepsilon_{12} = [(\varepsilon_I^{\,p} + \varepsilon_{12}^{\,e}) + \varepsilon_{12}^{\,+} t^n] + [-\varepsilon_{12}^{\,e}]$$

$$+ [-(\varepsilon_{12}^{\,e} + \varepsilon_{II}^{\,p}) - \varepsilon_{12}^{\,+}(t-t_1)^n] \quad ,$$

or $$\varepsilon_{12} = (\varepsilon_I^{\,p} - \varepsilon_{II}^{\,p} - \varepsilon_{12}^{\,e}) + \varepsilon_{12}^{\,+} t^n - \varepsilon_{12}^{\,+}(t-t_1)^n \quad , \quad t_1 \le t < t_2 \ , \ (3)$$

Phase III

$$\varepsilon_{12} = [(\varepsilon_I^{\,p} - \varepsilon_{II}^{\,p} - \varepsilon_{12}^{\,e}) + \varepsilon_{12}^{\,+} t^n - \varepsilon_{12}^{\,+}(t-t_1)^n] + [\varepsilon_{12}^{\,e}]$$

$$+ [(\varepsilon_{12}^{\,e} + \varepsilon_{III}^{\,p}) + \varepsilon_{12}^{\,+}(t-t_2)^n] \quad ,$$

or $$\varepsilon_{12} = (\varepsilon_I^{\,p} - \varepsilon_{II}^{\,p} + \varepsilon_{III}^{\,p} + \varepsilon_{12}^{\,e})$$

$$+ \varepsilon_{12}^{\,+} t^n - \varepsilon_{12}^{\,+}(t-t_1)^n + \varepsilon_{12}^{\,+}(t-t_2)^n \quad , \qquad t_2 \le t < t_3 \ , \ (4)$$

Phase IV

$$\varepsilon_{12} = (\varepsilon_I^{\,p} - \varepsilon_{II}^{\,p} + \varepsilon_{III}^{\,p} - \varepsilon_{IV}^{\,p} - \varepsilon_{12}^{\,e})$$

$$+ \varepsilon_{12}^{\,+} t^n - \varepsilon_{12}(t-t_1)^n + \varepsilon_{12}^{\,+}(t-t_2)^n - \varepsilon_{12}^{\,+}(t-t_3)^n \ , \ t_3 \le t < t_4 \ , \ (5)$$

Phase V

$$\varepsilon_{12} = (\varepsilon_I^p - \varepsilon_{II}^p + \varepsilon_{III}^p - \varepsilon_{IV}^p + \varepsilon_V^p + \varepsilon_{12}^e)$$
$$+ \varepsilon_{12}^+ t^n - \varepsilon_{12}(t-t_1)^n + \varepsilon_{12}^+(t-t_2)^n$$
$$- \varepsilon_{12}^+(t-t_3)^n + \varepsilon_{12}^+(t-t_4)^n \quad , \qquad t_4 \le t < t_5 \ , \ (6)$$

Phase VI

$$\varepsilon_{12} = (\varepsilon_I^p - \varepsilon_{II}^p + \varepsilon_{III}^p - \varepsilon_{IV}^p + \varepsilon_V^p - \varepsilon_{VI}^p - \varepsilon_{12}^e)$$
$$+ \varepsilon_{12}^+ t^n - \varepsilon_{12}(t-t_1)^n + \varepsilon_{12}^+(t-t_2)^n - \varepsilon_{12}^+(t-t_3)^n$$
$$+ \varepsilon_{12}^+(t-t_4)^n - \varepsilon_{12}^+(t-t_5)^n \quad , \qquad t_5 \le t \le t_6 \ , \ (7)$$

where $t_i$ , $i = 1 , \ldots , 6$ are given by 1007.3 hr., 1151.6 hr., 1319.4 hr., 1511.8 hr., 1655.5 hr., and 1846.1 hr., respectively; $n$ is 0.439, $\varepsilon_{12}^+$ is 0.0045 per cent/(hours)$^n$ , $\varepsilon^e$ is 0.0347 per cent and $\varepsilon_I^p , \ldots , \varepsilon_{VI}^p$ are as previously given. The fit of the experimental data to (2) through (7) shown in Fig. 8a is good.

Constitutive equations were developed in [7] for the time-dependent behavior of 304 stainless steel based on a strain-hardening model. Auxiliary rules were provided for situations involving stress reversals. If the constant stress creep data are represented by the power function, (1), and the reverse loadings in Test 8 are analyzed using the rules in [7], the following equations are obtained for "creep strains" $\varepsilon^c$ (total strain minus the elastic and plastic components):

Phase I $\qquad \varepsilon^c = \varepsilon_{12}^+ t^n \quad , \qquad t < t_1$

Phase II $\qquad \varepsilon^c = \varepsilon_{12}^+ t_1^n - \varepsilon_{12}^+(t-t_1)^n \quad , \qquad t_1 \le t < t_2$

Phase III $\qquad \varepsilon^c = \varepsilon_{12}^+ t_1^n - \varepsilon_{12}^+(t_2-t_1)^n + \varepsilon_{12}^+(t-t_2')^n \quad , \qquad t_2' < t_2 \le t < t_3$

**Phase IV**

$$\varepsilon^c = \varepsilon_{12}^{+} t_1^n - \varepsilon_{12}^{+}(t_2-t_1)^n + \varepsilon_{12}^{+}(t_3-t_2')^n - \varepsilon_{12}^{+}(t-t_3')^n \quad , \qquad t_3' < t_3 \leq t < t_4$$

**Phase V**

$$\varepsilon^c = \varepsilon_{12}^{+} t_1^n - \varepsilon_{12}^{+}(t_2-t_1)^n + \varepsilon_{12}^{+}(t_3-t_2')^n - \varepsilon_{12}^{+}(t_4-t_3')^n + \varepsilon_{12}^{+}(t-t_4')^n \quad , \qquad t_4' < t_4 \leq t < t_5$$

**Phase VI**

$$\varepsilon^c = \varepsilon_{12}^{+} t_1^n - \varepsilon_{12}^{+}(t_2-t_1)^n + \varepsilon_{12}^{+}(t_3-t_2')^n - \varepsilon_{12}^{+}(t_4-t_3')^n + \varepsilon_{12}^{+}(t_5-t_4')^n - \varepsilon_{12}^{+}(t-t_5')^n \quad , \qquad t_5' < t_5 \leq t < t_6 \qquad (8)$$

where

$$t_2' = t_2 - \left[\left(\varepsilon_{12}^{+} t_1^n - \varepsilon_{12}^{+}(t_2-t_1)^n\right)/\varepsilon_{12}^{+}\right]^{1/n*}$$

$$= t_2 - \left(t_1^n - (t_2-t_1)^n\right)^{1/n} \quad ,$$

$$t_3' = t_3 - \left[\left(\varepsilon_{12}^{+} t_1^n - \varepsilon_{12}^{+}(t_3-t_2')^n\right)/\varepsilon_{12}^{+}\right]^{1/n**}$$

$$= t_3 - \left(t_1^n - (t_3-t_2')^n\right)^{1/n} \quad .$$

Similarly

$$t_4' = t_4 - \left(t_1^n - (t_4-t_3')^n\right)^{1/n} \quad ,$$

and

$$t_5' = t_5 - \left(t_1^n - (t_5-t_4')^n\right)^{1/n} \quad . \qquad (9)$$

---

*Since the final strain in Phase I is greater than zero, hardening, equal to the creep strain accumulated in Phase I minus the absolute value of the creep strain accumulated in Phase II, occurs in positive loadings (Phase II).

**Since the final strain is less than the largest strain $\varepsilon^{+} t_1^n$, hardening, equal to the creep accumulated in Phase II minus the creep accumulated in Phase III, occurs in negative loadings in Phase IV (i.e., hardening equal to $\varepsilon^{+} t_1^n$ minus $\varepsilon_{12}^{+}(t_3-t_2')$ occurs).

Since equations (8) apply only for "creep strains," the creep data shown in Fig. 8a was changed into "creep strains" by subtracting the first strain reading in each phase from the remaining data in that phase. The results of this modification and the curves for (8) are shown in Fig. 8b. Comparing Fig. 8a and 8b the former shows a much better fit to the data.

Yield Surface Subsequent to Long-time Creep

An attempt was made to determine a few points on the yield curve subsequent to the creep test programs of Test 4 in order to evaluate the problems of making such determinations. Only two probes were made before the lead wire to the lamp burned out, necessitating dismantling the specimen. Tensile loads were first applied in increments starting at 6600 psi. After each load was applied and strain measured, the load was returned to a reference loading to check for permanent strains.

Selecting the yield criterion corresponding to the first occurrence of 10μ in./in. offset strain, the yield point in tension determined after Test No. 4P was between 11,920 psi and 12,455 psi in conjunction with a small shear stress ($\tau$ = 1833 psi) . The associated total offset strains were 8μ in./in. and 25μ in./in., respectively. However, because the offset strains showed some scatter, loadings were continued up to $\sigma$ = 17,231 psi.

A similar procedure was then used in pure torsion. However, the starting load was too high, resulting in yielding on the second loading and possibly the first. The first loading was at $\tau$ = 7611 psi . The second loading was at $\tau$ = 8754 psi and produced a 25μ in./in. offset with respect to the first loading. The highest stress used in this probe was 11,612 psi. After unloading the procedure was repeated in torsion with the result that the yield stress then appeared to be between 6406 psi and 6978 psi (9 and 13μ in./in. offset, respectively).

After Test No. 5G probes were made at temperature to determine a few points on the 1100°F yield curve subsequent to the stress history shown in Table VII. (The last loading in this history was a tension creep test at 15 ksi for 19.35 hours.) Stresses were added in increments starting from a value of stress which was in the elastic zone where creep behavior did not occur. After each load was applied and strain was measured, the load was returned quickly to the reference load to check for permanent plastic strains. The yield criterion selected was the first occurrence of about 10μ in./in. effective offset strain. The results of the probes following this procedure are shown in Fig. 11. The results seem consistent and suggest that the technique may be employed to study the effect of creep straining on the yield surface at elevated temperatures.

Circumferential Strains

Attempts to measure the circumferential strains during creep testing at elevated temperatures were made in Tests 5 through 9. The initial circumferential extensometer which was used is discussed on page 25. In Test No. 5 this extensometer did not function properly. In Test No. 6 the performance of a modified extensometer was satisfactory. The data from the circumferential extensometer in Test No. 6 for the 1000 hours of creep is shown in Fig. 12. Circumferential strains observed (for creep and recovery) in Test No. 7 are shown in Fig. 12 also. Strains during the early part of the test are not available due to a circuitry error, which also affected the zero reading. Thus the strains shown are approximations which were computed by selecting a zero reading which would yield the same ratio of axial to circumferential strain at 300 hr. in Test No. 7 as observed in the pure tension creep test at 300 hr. in Test No. 6. In this computation it was assumed for simplicity that Test No. 7 was under a uniaxial stress. Circumferential strains in Test No 8, a test in pure torsion at an effective Mises stress of 10 ksi, were observed but were so small that strains were due primarily to thermal fluctuations.

There appeared to be no real circumferential strains for Test No. 8.

In Test No. 9, a pure tension test at 10 ksi effective Mises stress, circumferential strains were observed. However, the trend in the circumferential strains was not consistent with the axial strains (i.e., $\varepsilon_{22} = -\nu\varepsilon_{11}$) throughout the creep test. Because the axial strains were small (less than 0.2 per cent), the circumferential strains should also be small. Since the average temperature in this test monotonically increased 9.7°F from the start of the test to 1008.2 hours, thermal strains developed in the specimen and appeared in the circumferential strain readings. The effect of these thermal strains was to cause the small circumferential strain readings, which should increase negatively with time, to increase positively with time (i.e., the temperature effect masked the true strain readings). Some data obtained during the early part of Test No. 9, when the temperature drift was small, are given in Table XII.

## Poisson's Ratio vs. Time

The only reliable source that provides information on the behavior of Poisson's ratio with respect to time is Test No. 6, Fig. 12. The data for this test indicate an initial Poisson's ratio of 0.31 increasing gradually during creep to 0.38 at 500 hr., based on total strain, which seems reasonable. It is noteworthy that the circumferential strain rate increased more rapidly than the axial strain beginning at 500 hr. The circumferential strain is measured at only one cross section near the upper end of the specimen, whereas the axial strain is averaged over 4 in.

## Elastic Moduli

The elastic modulus $E$ at 1112°F was determined from the slope of the unloading curve obtained during the tensile yield point determinations in Test No. 4. The value obtained was $19.7 \times 10^6$ psi. In this determination the effect

of the small torque (1833 psi) was not accounted for. The shear modulus G at 1110°F was determined at $9.8 \times 10^6$ psi from the slope of the unloading curve of a torsional yield-point probe. Poisson's ratio determined from the total strains in the early stage of tensile creep at 15 ksi was found to be 0.31 at 1096°F in Test No. 6. This observation undoubtedly includes some plastic strain, however.

Similarly, the elastic modulus E at 1107°F was determined in yield-point probes in Test No. 5 from the slope of the unloading curve at $20.6 \times 10^6$ psi ($20.4 \times 10^6$ psi for the loading curve); and the shear modulus G at 1109°F was determined to be $7.3 \times 10^6$ psi from a loading curve.

Elastic moduli determined from recovery tests as described on page 13 are given in Table X.

### Third Stage Creep at Small Stress and Strain

As reported on page 3, Test No. 6 clearly entered the third stage of creep after about 500 hours under a pure tension stress of 15 ksi and at a total strain of about 1 per cent. All indications are that accelerating creep was well under way while the temperature was still normal. This observation that third stage behavior can initiate at such small stresses, strains and times is rather disturbing. Consequently, this experiment is being repeated.

## APPARATUS AND TEST PROCEDURE

### Lamp Life

The problem of failure of the quartz tube heating lamp, used as the primary source of heat, at less than 1000 hr. appears to have been solved starting with Test 4. Previous lamp failures occurred at the upper lead seal. By water cooling the upper pull rod adaptor which enclosed the end of the lamp, the lamp life has been extended to more than 2600 hr. No lamp failures have occurred since Test 4.

## Temperature Control and Measurement

The upward drift of temperature during a creep test and the deviation of temperature from the desired value have received considerable attention. Possible sources of drift and means of determining the probable cause have been considered. No means of establishing the cause has been found. Among the possibilities are: gradual deterioration of the lamp, gradual deterioration of the end heaters and drift of the Thermac controller. The manufacturers assure us that the Thermacs do not drift. We have not found a way to prove this. One lamp showed considerable film deposits in the vicinity of the spacers. This lamp, used in Test No. 5, had been heated to 1111°F for 2808 hr.

In Tests 4 through 9 one thermocouple at the center of the specimen was selected as the reference couple and its temperature adjusted to 1100°F. Then the distribution was adjusted to minimize the variation among couples. As a result the average reading of all thermocouples subsequently reported differed from the initial setting. This procedure has been changed so that the variation is made as small as possible and then the average of all thermocouples is adjusted to the desired temperature at the beginning of the test. After the start of a test the temperature has not been readjusted. There seems no way to tell whether the drift is in the control couple, the controller, the heaters or the other measuring couples.

To minimize the chance of losing a test due to burn out of the control thermocouple which is located on the inside wall of the specimen, two control couples were located adjacent to each other and wired in parallel.

## Accommodation of Large Torsional Strains

The creep strains in some tests involving torsion were larger than expected and exceeded the limit of travel of the extensometer as constrained by

the many other items attached to the specimen. This problem has been eliminated by changing the shape of one of the extensometer rods.

## Circumferential Extensometer

The development of a circumferential extensometer initiated in the first year was continued. In Test 5 a pair of DCDT's were mounted on a pair of invar rods attached at their midpoint to the thermal shield around the specimen. The DCDT's were mounted on opposite sides of the specimen and their cores were fitted with nicrome-wire probes to measure the displacement of two opposing points on the outside diameter of the specimen. The probes were spot welded to the specimen on one end and engaged a socket on the transducer on the other end. This system did not work.

A second circumferential extensometer was used in Test No. 6. The following modifications were made to correct suspected difficulties in the first instrument. The probe wires were mounted by welding to the specimen using an insulated C-shaped guide for accurate positioning. Friction causing separation of the probe wire and socket seems the most likely explanation of poor performance of the first model, in spite of jeweled bearings in the DCDT's. Accordingly, the probe wires were attached firmly to the DCDT's by means of set screws. Results show a typical creep curve. However, the sensitivity of this instrument is less than that of the axial extensometer, and it is more temperature sensitive. Alignment of the probes is very difficult. It is felt that this may be more significant in limiting the accuracy than sensitivity to strain and temperature. It was planned to use two sets of DCDT's to sense the change in two diameters at right angles. However, it appears almost impossible to assemble this extra complexity. The performance of this instrument seems to be satisfactory.

## Uniaxial Creep Machine

A uniaxial creep machine was instrumented with an axial and a circumferential extensometer. The former is the same as that used for combined tension and torsion, except that the drum and pointer for twist measurement were omitted. The latter was the same as used on the combined tension and torsion testing machine.

## Compression Creep Apparatus

One of the problems in developing this apparatus is the possibility of buckling. A means of reducing the chance of buckling by shortening the total length of the specimen-and-grip system was explored. A short (8-13/16 in.) heating lamp was obtained. This lamp had a lower wattage than those currently in use. The lamp was mounted in an old specimen with suitable shortened end fittings, end heaters, thermocouples and a heat reflector. Then a test was made to determine whether it would be possible to use this lamp in tests at 1100°F. Results indicate that the lamp has sufficient wattage but little to spare. So the method appears possible. Some preparations were made toward performing a compression load test on this system at temperature to determine whether buckling is likely at stresses up to 15,000 psi.

## ACKNOWLEDGMENT

The authors thank Professor D. H. Avery for help with metallurgical questions and Messrs. R. A. Moio, P. Previte and H. R. Frederick for assistance in starting up tests.

## REFERENCES

1. Findley, W. N., and Mark, R., "Multiaxial Creep Behavior of 304 Stainless Steel," Annual Report No. 1, Contract 3599, Union Carbide Corporation, October 1972.

2. Blass, J. J., and Findley, W. N., "Short-Time Biaxial Creep of an Aluminum Alloy with Abrupt Changes of Temperature and State of Stress," Transactions, ASME, Journal of Applied Mechanics, Vol. 38, Series E, No. 2, June 1971, pp. 489-501.

3. Findley, W. N., and Lai, J. S. Y., "A Modified Superposition Principle Applied to Creep of Nonlinear Viscoelastic Material under Abrupt Changes in State of Combined Stress," Transactions of the Society of Rheology, Vol. 11, Part 3, 1967, pp. 361-380.

4. Wang, T. T., and Onat, E. T., "Nonlinear Mechanical Behavior of 1100 Aluminum at 300°F," Acta Mech., 5, 1968, pp. 54-70.

5. Lubahn, J. D., "Deformation Phenomena," Mechanical Behavior of Materials at Elevated Temperatures, J. E. Dorn (ed.), McGraw-Hill, 1961, pp. 319-92.

6. Greenstreet, W. L., Corum, J. M., Pugh, C. E., "High-Temperature Structural Design Methods for LMFBR Components, Quarterly Progress Report for Period Ending December 31, 1971," USAEC Report ORNL-TM-3736, Oak Ridge National Laboratory, March 1972.

7. Pugh, C. E., Liu, K. C., Corum, J.M., Greenstreet, W. L., "Currently Recommended Constitutive Equations for Inelastic Design Analysis of FFTF Components," USAEC Report ORNL-TM-3602, September 1972.

MCG

Table I

Creep Experiments on 304 Stainless Steel

| Test Number | Specimen Number | Date of Start of Test | Tensile Stress, Psi | Shear Stress, Psi | Effective Stress, Ksi | Total Duration of Test at Constant Stress and Temp., hr. | Average Temperature, °F | Long-term Drift,* °F |
|---|---|---|---|---|---|---|---|---|
| 1 | 1-304-16 | 5-2-72 | 10,628 | 6,111 | 15 | 1003.0 | 1105 | +7 |
| 2 | 2-304-16 | 7-13-72 | 13,975 | 3,407 | 15.17 | 152.5 | 1100 | +5 |
| 3 | 5-304-16 | 7-27-72 | 5,570 | 7,934 | 14.83 | 839.0 | 1100 | +16.1 |
| 4 | 9-304-16 | 10-18-72 | 0 | 10,493 | 18.175 | 1009.25 | 1107 | +6.0 |
| 5 | 6-304-16 | 11-8-72 | 10,628 | 6,111 | 15 | 1008.7 | 1111 | -0.3 |
| 6 | 12-304-16 | 11-5-72 | 15,000 | 0 | 15 | 601.1 | 1097 | +0.8 |
| 7 | 4-304-16 | 3-20-73 | 13,819 | 3,369 | 15 | 1006.9 | 1117 | +12.0 |
| 8 | 11-304-16 | 6-12-73 | 0 | 5,773 | 10 | 1007.0 | 1111 | +4.6 |
| 9 | 8-304-16 | 6-13-73 | 10,000 | 0 | 10 | 1008.2 | 1090 | +9.7 |
| 10 | 3-304-16 | - | 15,000 | 0 | 15 | - | - | - |
| 11 | 7-304-16 | 9-18-73 | - | 8,660 | 15 | - | - | - |

*Determined from initial and final temperature readings.

General Notes: 1) Data in Tests 1 to 9 are shown in Fig. 1 to 9, respectively.

2) Temperatures measured in Tests 1 and 2 were made with a strip chart recorder in conjunction with a L & N potentiometer. All other tests utilized a Doric temperature indicator.

Table II

Strain and Strain Rates

| Test No. | Tensile Stress, Psi | Torsional Stress, Psi | Effective Mises Stress, Psi | Strain at 1 hr., % | | Strain at 120 hr., % | | Effective Strain at 1 hr., % | Effective Strain at 120 hr., % | Difference in Effective Strain from 1 to 120 hr., % | Creep Rate, (Slope of Curve) at 120 hr., % per hr. | |
|---|---|---|---|---|---|---|---|---|---|---|---|---|
| | | | | $\varepsilon_{11}$ | $\varepsilon_{12}$ | $\varepsilon_{11}$ | $\varepsilon_{12}$ | | | | $\dot{\varepsilon}_{11}$ | $\dot{\varepsilon}_{12}$ |
| 1 | 10,628 | 6,111 | 15,000 | 0.3532 | 0.2863 | 0.5863[b] | 0.5075[b] | 0.4059 | 0.7044 | 0.2985 | 0.0006 | 0.0006 |
| 2 | 13,975 | 3,407 | 15,170 | 0.8786 | 0.4332 | 2.9140[a] | 1.1730[a] | 0.7703 | 2.3682 | 1.5979 | 0.0167 | 0.0051 |
| 3 | 5,570 | 7,934 | 14,830 | 0.3129 | 0.6369 | 0.5127 | 1.0720 | 0.7644 | 1.2842 | 0.5198 | 0.0006 | 0.0012 |
| 4[c] | 0 | 10,493 | 18,175 | -0.0123 | 1.0682 | -0.0095[b] | 1.9107[b] | 1.2335 | 2.2063 | 0.9728 | - | 0.0028 |
| 5 | 10,628 | 6,111 | 15,000 | 0.7230 | 0.6708 | 1.0562 | 0.9903 | 0.9122 | 1.3429 | 0.4307 | 0.0009 | 0.0010 |
| 6 | 15,000 | 0 | 15,000 | 0.4155 | - | 0.7838 | - | 0.2770 | 0.5225 | 0.2455 | 0.0009 | - |
| 7 | 13,819 | 3,369 | 15,000 | 0.9669 | 0.3512 | 1.4206 | 0.5454 | 0.7616 | 1.1373 | 0.3757 | 0.0015 | 0.0007 |
| 8 | 0 | 5,773 | 10,000 | 0.0001 | 0.0763 | -0.0122[b] | 0.1100[b] | 0.0881 | 0.1273 | 0.0392 | - | 0.0001 |
| 9 | 10,000 | 0 | 10,000 | 0.1065 | - | 0.1275[b] | - | 0.0710 | 0.0850 | 0.0140 | 0.0001 | - |
| 10 | 15,000 | 0 | 15,000 | To be completed | | | | | | | | |
| 11 | 0 | 8,660 | 15,000 | 0.0213 | 0.4343 | -0.0003[b] | 0.8846[b] | 0.5017 | 1.0214 | 0.5197 | - | 0.0016 |

[a] Extrapolated.

[b] Interpolated.

[c] Shear strains shown neglect the strains resulting from 1833 psi.

Table III

Fit of Experimental Data to $\varepsilon_{ij} = \varepsilon_{ij}^{o} + \varepsilon_{ij}^{+} t^{n}$, via Least Squares Fit, of the Primary Creep

| Test No. | Tensile Strain $\varepsilon_{11} = \varepsilon_{11}^{o} + \varepsilon_{11}^{+} t^{n}$, Per cent | Shear Strain $\varepsilon_{12} = \varepsilon_{12}^{o} + \varepsilon_{12}^{+} t^{n}$, Per cent | Maximum Time Considered, $t_{max}$, hr. | | RMS, per cent* | |
|---|---|---|---|---|---|---|
| | | | $\varepsilon_{11}$ | $\varepsilon_{12}$ | $\varepsilon_{11}$ | $\varepsilon_{12}$ |
| 1 | $0.2150 + 0.1422t^{0.195}$ | $0.1655 + 0.1244t^{0.195}$ | 1002.5 | 1002.5 | 0.0073 | 0.0069 |
| 2 | $0.5395 + 0.3339t^{0.321}$ | $0.1294 + 0.3108t^{0.134}$ | 75.3 | 24.0 | 0.0072 | 0.0168 |
| 3 | $0.2356 + 0.0711t^{0.289}$ | $0.4742 + 0.1567t^{0.309}$ | 579.0 | 73.9 | 0.0078 | 0.0101 |
| 4 | - | $0.8184 + 0.2387t^{0.326}$ | - | 548.35 | - | 0.0320 |
| 5 | $0.6323 + 0.0693t^{0.383}$ | $0.6026 + 0.0574t^{0.402}$ | 1008.7 | 1008.7 | 0.0195 | 0.0173 |
| 6 | $0.2576 + 0.1635t^{0.240}$ | - | 571.9 | - | 0.0080 | - |
| 7 | $0.8010 + 0.1488t^{0.312}$ | $0.2937 + 0.0531t^{0.337}$ | 527.1 | 479.0 | 0.0215 | 0.0080 |
| 8 | - | $0.0725 + 0.0045t^{0.439}$ | - | 1007.0 | - | 0.0013 |
| 9 | $0.0999 + 0.0066t^{0.284}$ | - | 1008.2 | - | 0.0017 | - |

*Based on times up to $t_{max}$.

Table IV

History of Initial Plastic Straining in Test No. 1 at Room Temperature

| Stress State, $(\sigma;\tau)$, psi | Duration | Total Plastic Strain Accumulated, % | |
|---|---|---|---|
| | | $\varepsilon_{11}$ | $\varepsilon_{12}$ |
| (10628;6111) | 1 min. | -* | .0054 |
| (10628;6111) | 7 min. | .0036+ | .0070 |
| (0;0) | ∿24 hrs. | .0043+ | .0070 |
| (10628;6111) | 4 min. | .0067+ | .0074 |
| (0;0) | ∿22.25 hrs. | .0088+ | .0074 |
| (10628;6111) | 4.75 min. | .0097+ | .0083 |

*Lost zero reading.

+To these figures should be added the plastic strain occurring on first loading which is not known.

Table V. Hardness Tests

| Specimen Number | Condition | Location | Rockwell Hardness |
|---|---|---|---|
| Bar No. 16 | As received | | C 35 |
| 1-304-16 | After creep test | Shoulder | B 69 |
| 2-304-16 | " " " | " | B 67 |
| 5-304-16 | " " " | " | B 62 |
| 12-304-16 | " " " | " | B 68 |
| 2-304-16 | " " " | Test section | A 46 |
| 12-304-16 | " " " | " " | A 44 |
| Bar No. 16 | Chips: Machined and heat treated with following time at temperature of 2000°F | | |
| | 30 min. | | A 37 |
| | 45 min. | | A 37 |
| | 60 min. | | A 40 |
| | 75 min. | | A 39 |
| | 90 min. | | A 37 |
| | 105 min. | | A 38 |
| | 120 min. | | A 37 |
| | 135 min. | | A 37 |

Table VI

Supplementary Program of Test No. 4, Specimen 9-304-16

| Test No. | Stress State ($\sigma;\tau$), Psi | Duration, Hr. | Initial* Strain, Per cent | | Final Strain, Per cent | |
|---|---|---|---|---|---|---|
| | | | $\varepsilon_{11}$ | $\varepsilon_{12}$ | $\varepsilon_{11}$ | $\varepsilon_{12}$ |
| 4A | (0;-6,827) | 48.30 | - | 3.4575 at 10 sec. | - | 3.3706 |
| 4B | (0;+10,618) | 71.35 | - | 3.5185 at 7 sec. | - | 3.6911 |
| 4C | (0;-6,827) | 48.00 | - | 3.5719 at 10 sec. | - | 3.4874 |
| 4D | (0;+10,493) | 48.00 | - | 3.6207 at 5 sec. | - | 3.7613 |
| 4E | (0;+1,833) | 91.80 | - | 3.7198 at 15 sec. | - | 3.7099 |
| 4F | (0;-6,827) | 24.90 | - | 3.6486 at 15 sec. | - | 3.5909 |
| 4G | (0;+1,833) | 18.65 | - | 3.6384 at 6 sec. | - | 3.6486 |
| 4H | (0;-6,827) | 28.75 | - | 3.6019 at 27 sec. | - | 3.5762 |
| 4I | (0;+1,833) | 71.70 | - | 3.6256 at 9 sec. | - | 3.6371 |
| 4J | (15,000;+1,833) | 47.90 | 0.0730 at 20 sec. | 3.6399 at 40 sec. | 0.1052 | 3.6468 |
| | Raise temperature 1111°F to 1170°F. | | | | | |
| 4K | (15,000;+1,833) | 187.75 | 0.1652 at 15 sec. | 3.6510 at 15 sec. | 0.5387 | 3.7046 |
| | Lower temperature 1170°F to 1110°F | | | | | |
| 4L | (15,000;+1,833) | 168.05 | 0.4767 at 15 sec. | 3.7013 at 12 sec. | 0.5251 | 3.7070 |
| 4M | (0;+1,833) | 124.50 | 0.4526 at 15 sec. | 3.7123 at 1 min. 7 sec. | 0.4388 | 3.7128 |
| 4N | (15,000;+1,833) | 143.90 | 0.5113 at 10 sec. | 3.7080 at 4 min. | 0.5379 | 3.7112 |
| 4P | (0;+1,833) | 235.50 | 0.4646 at 15 sec. | 3.7133 at 3 min. | 0.4536 | 3.7129 |
| | Subsequent Yield Point Probes | | | | | |

*First observation after change in load.

Table VII

Supplementary Program of Test No. 5, Specimen 6-304-16

| Test No. | Stress State ($\sigma;\tau$), Psi | Duration, Hr. | Initial Strain, Per cent | | Final Strain, Per cent | |
|---|---|---|---|---|---|---|
| | | | $\varepsilon_{11}$ | $\varepsilon_{12}$ | $\varepsilon_{11}$ | $\varepsilon_{12}$ |
| 5A | (0;0) | 1127.00 | 1.5895 at 20 sec. | 1.5139 at 12 sec. | 1.5595 | 1.4979 |
| 5B | (10,628;6,111) | 2.25 | 1.5739 at 10 sec. | 1.5392 at 37 sec. | 1.6172 | 1.5438 |
| 5C | (0;0) | 18.00 | 1.5657 at 60 sec. | 1.5042 at 90 sec. | 1.5628 | 1.5006 |
| 5D | (0;8,660) | 6.5 | 1.5618 at 10 sec. | 1.5600 at 13 sec. | 1.5610 | 1.5722 |
| 5E | (0;0) | 21.6 | 1.5610 at 15 sec. | 1.5162 at 20 sec. | 1.5586 | 1.5111 |
| 5F | (15,000;0) | 19.35 | 1.6360 at 15 sec. | 1.5102 at 48 sec. | 1.6578 | 1.5098 |
| 5G | (0;0) | 168.35 | 1.5848 at 15 sec. | 1.5095 at 36 sec. | 1.5749 | 1.5073 |
| | | Subsequent Yield Surface Probes | | | | |

Table VIII

Supplementary Program of Test No. 8, Specimen 11-304-16

| Test No. | Stress State ($\sigma;\tau$), Psi | Duration, Hr. | Initial Strain, Per cent | | Final Strain, Per cent | |
|---|---|---|---|---|---|---|
| | | | $\epsilon_{11}$ | $\epsilon_{12}$ | $\epsilon_{11}$ | $\epsilon_{12}$ |
| 8A | (0;-5773) | 143.5 | - | 0.0423 at 15 sec. | - | 0.0129 |
| 8B | (0;+5773) | 167.3 | - | 0.1185 at 10 sec. | - | 0.1493 |
| 8C | (0;-5773) | 191.4 | - | 0.0408 at 15 sec. | - | 0.0056 |
| 8D | (0;+5773) | 142.3 | - | 0.1045 at 10 sec. | - | 0.1406 |
| 8E | (0;-5773) | 191.6 | - | 0.0383 at 13 sec. | - | 0.0029 |

Table IX

Supplementary Program of Test No. 9, Specimen 8-304-16

| Test No. | Stress State ($\sigma;\tau$), Psi | Duration, Hr. | Initial Strain, Per cent | | Final Strain, Per cent | |
|---|---|---|---|---|---|---|
| | | | $\varepsilon_{11}$ | $\varepsilon_{12}$ | $\varepsilon_{11}$ | $\varepsilon_{12}$ |
| 9A | (0;0) | 647.8 | 0.1025 at 23 sec. | - | 0.0849 | - |
| 9B | (10,000;0) | 46.3 | 0.1318 at 15 sec. | - | 0.1370 | - |
| 9C | (0;0) | 23.8* | 0.0899 at 10 sec. | - | 0.0884 | - |
| 9D | (10,000;0) | 66.3 | 0.1353 at 5 sec. | - | 0.1388 | - |
| | | | Raise temperature 24.2°F. | | | |
| 9E | (10,000;0) | 47.6 | 0.1523 at 60 sec. | - | 0.1490 | - |
| | | | Lower temperature 32.1°F. | | | |
| 9F | (10,000;0) | 192.2 | 0.1037 at 25 sec. | - | 0.1390 | - |
| | | | Raise temperature 24.1°F. | | | |
| 9G | (10,000;0) | 317.9 | 0.1844 at 60 sec. | - | 0.1891 | - |

*Approximate time.

Table X

Fit of Experimental Data to
$\varepsilon_{ij} = \varepsilon_{ij}^{o} + \varepsilon_{ij}^{+} t^{n}$ via
Least Squares Fit of Recovery

| Test No. | Tensile Strain $\varepsilon_{11} = \varepsilon_{11}^{o} + \varepsilon_{11}^{+} t^{n}$,* Per cent | Shear Strain $\varepsilon_{12} = \varepsilon_{12}^{o} + \varepsilon_{12}^{+} t^{n}$,* Per cent | Error in RMS, Per cent** | | E, Psi × $10^6$ | G, Psi × $10^6$ |
|---|---|---|---|---|---|---|
| | | | $\varepsilon_{11}$ | $\varepsilon_{12}$ | | |
| 5A | $-0.0499 - 0.0020t^{0.386}$ | $-0.0129 - 0.0250t^{0.05}$ | 0.0011 | 0.0003 | - | - |
| 5C | $-0.0479 - 0.0050t^{0.08}$ | $-0.0148 - 0.0269t^{0.02}$ | 0.0002 | 0.0002 | - | - |
| 5E | $0.0 - 0.0002t^{0.81}$ | $-0.0549 - 0.0033t^{0.211}$ | 0.0002 | 0.0001 | - | 7.89 @ 1109.2°F |
| 5G | $-0.0655 - 0.0107t^{0.08}$ | $-0.0005 - 0.0004t^{0.33}$ | 0.0005 | 0.0002 | 22.9 @ 1106.9°F | - |
| 7A | $-0.0584 - 0.0128t^{0.155}$ | $-0.0241 - 0.0090t^{0.084}$ | 0.0005 | 0.0004 | - | - |
| 9A | $-0.0464 - 0.0004t^{0.602}$ | - - - | 0.0004 | - | 21.6 @ 1096.2°F | - |
| 9C | $-0.0469 - 0.0005t^{0.382}$ | - - - | 0.0001 | - | 21.3 @ 1097.2°F | - |

* $\varepsilon_{ij}^{o}$ shown in the table was obtained by subtracting the last strain reading recorded before recovery from the value of A obtained by the least squares fit of the test data to $\varepsilon_{ij} = A + \varepsilon_{ij}^{+} t^{n}$.

** All data considered.

Table XI

Effect of Temperature on Creep Rate
with the Tensile Stress held
Constant at 10 ksi

| Test No. | Average Temperature, °F | Change in Temperature,* °F | Creep Rate, %/hr. |
|---|---|---|---|
| 9D | 1097.9 | 0 | 0.00004 at 66.3 hr. |
| 9E | 1122.1 | +24.2 | 0.00014 at 30.7 hr. |
| 9F | 1065.8 | -32.1 | 0.00001 at 47.4 hr. |
| 9G | 1122.0 | +24.1 | 0.00014 at 95.8 hr. |

*With respect to 1097.9°F (Test 9D).

Table XII

Circumferential Strains in Test No. 9

| Time, hr. | Temperature, °F | $\varepsilon_{11}$, % | $-\varepsilon_{22}$, % | $\nu$ |
|---|---|---|---|---|
| 0 | 1085.5 | 0 | 0 | - |
| 0.007 | 1087.7* | 0.1017 | 0.0322 | 0.32 |
| 0.067 | 1085.3 | 0.1027 | 0.0275 | 0.27 |
| 0.25 | 1084.8 | 0.1047 | 0.0307 | 0.29 |
| 3.5 | 1085.6 | 0.1097 | 0.0366 | 0.33 |
| 24.4 | 1085.6 | 0.1172 | 0.0340 | 0.29 |

*Less one additional thermocouple reading.

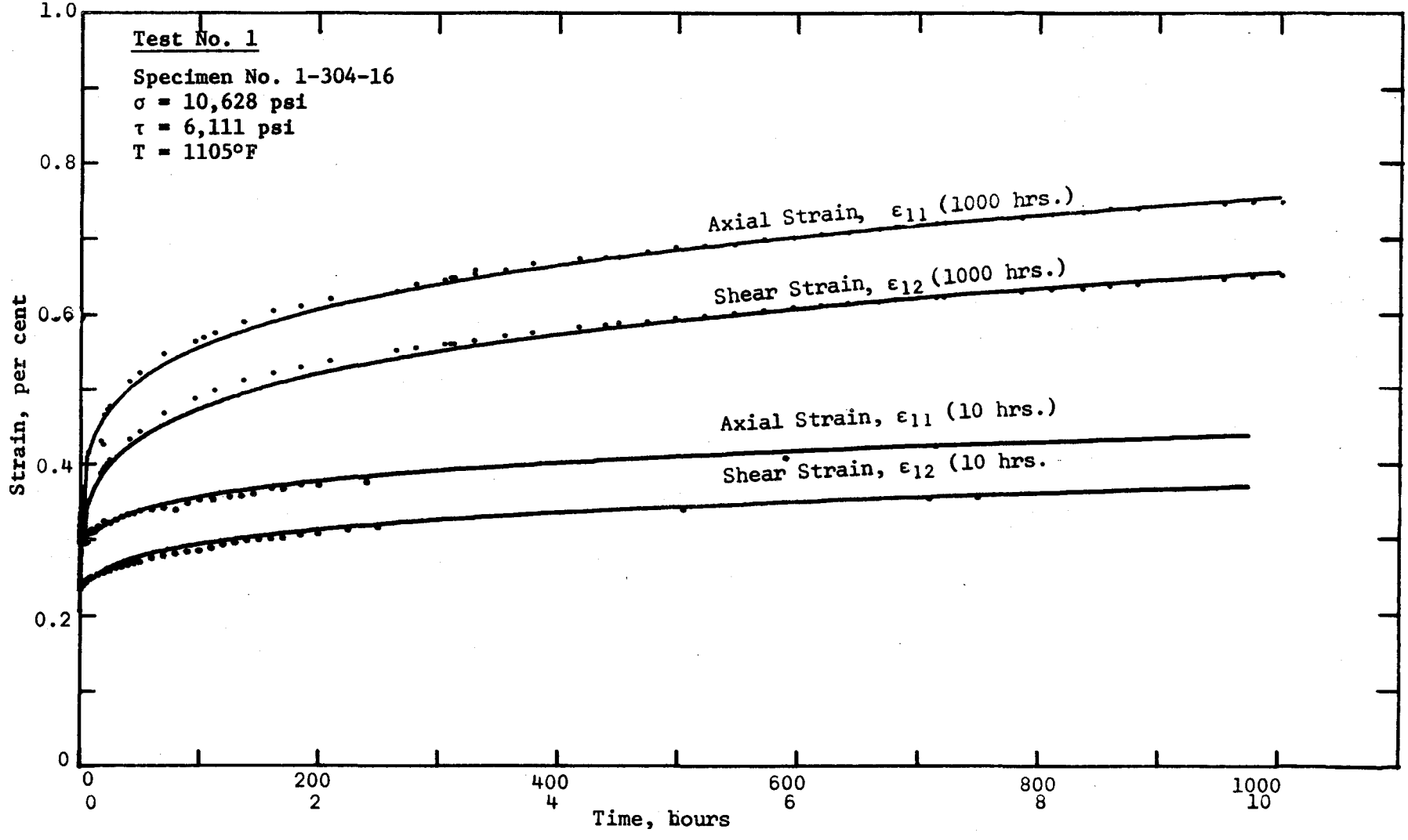


Fig. 1. Total Strain vs. Time during Constant Load Creep.

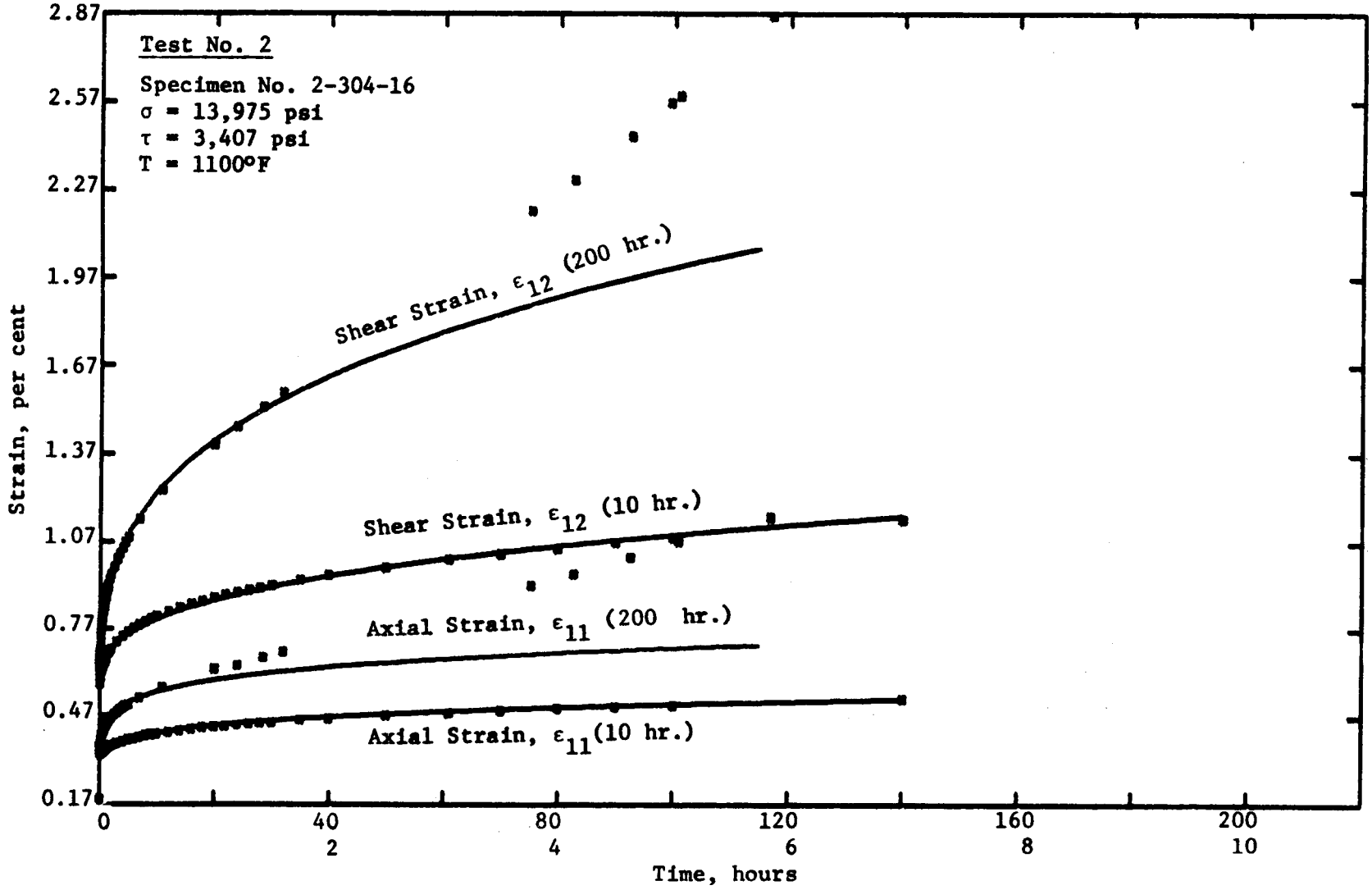


Fig. 2. Total Strain vs. Time during Constant Load Creep.

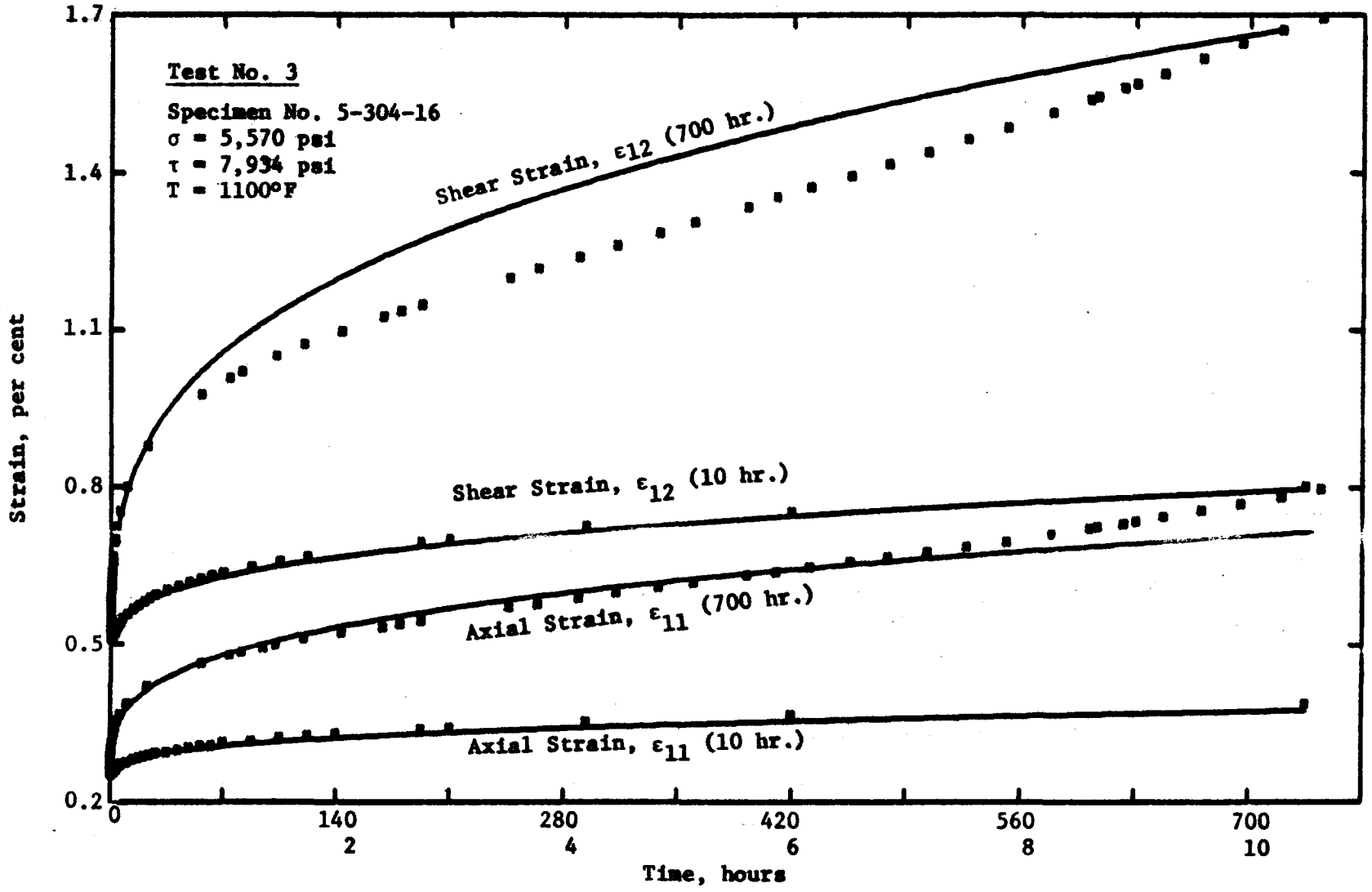


Fig. 3. Total Strain vs. Time during Constant Load Creep.

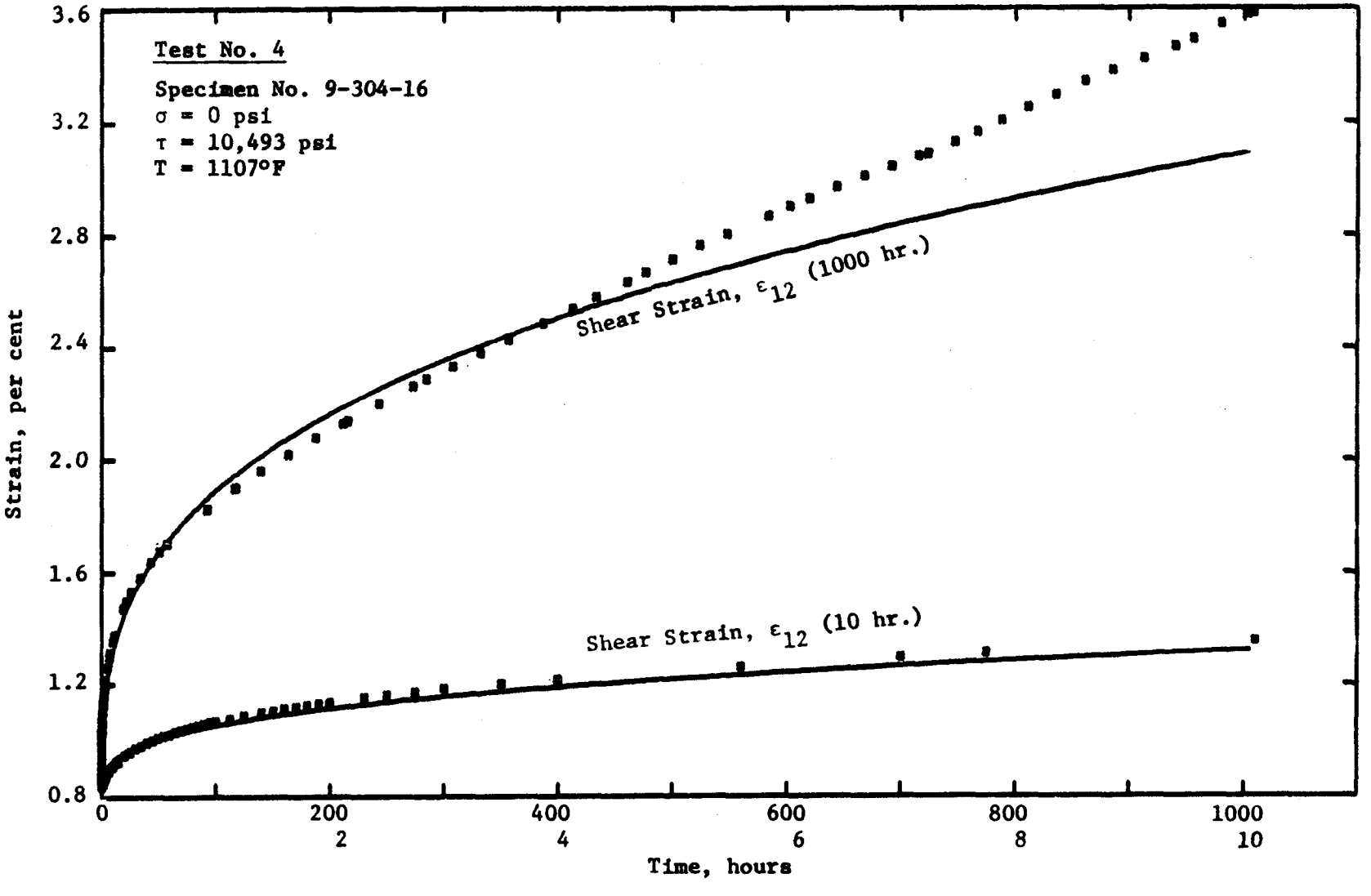


Fig. 4. Total Strain vs. Time during Constant Load Creep.

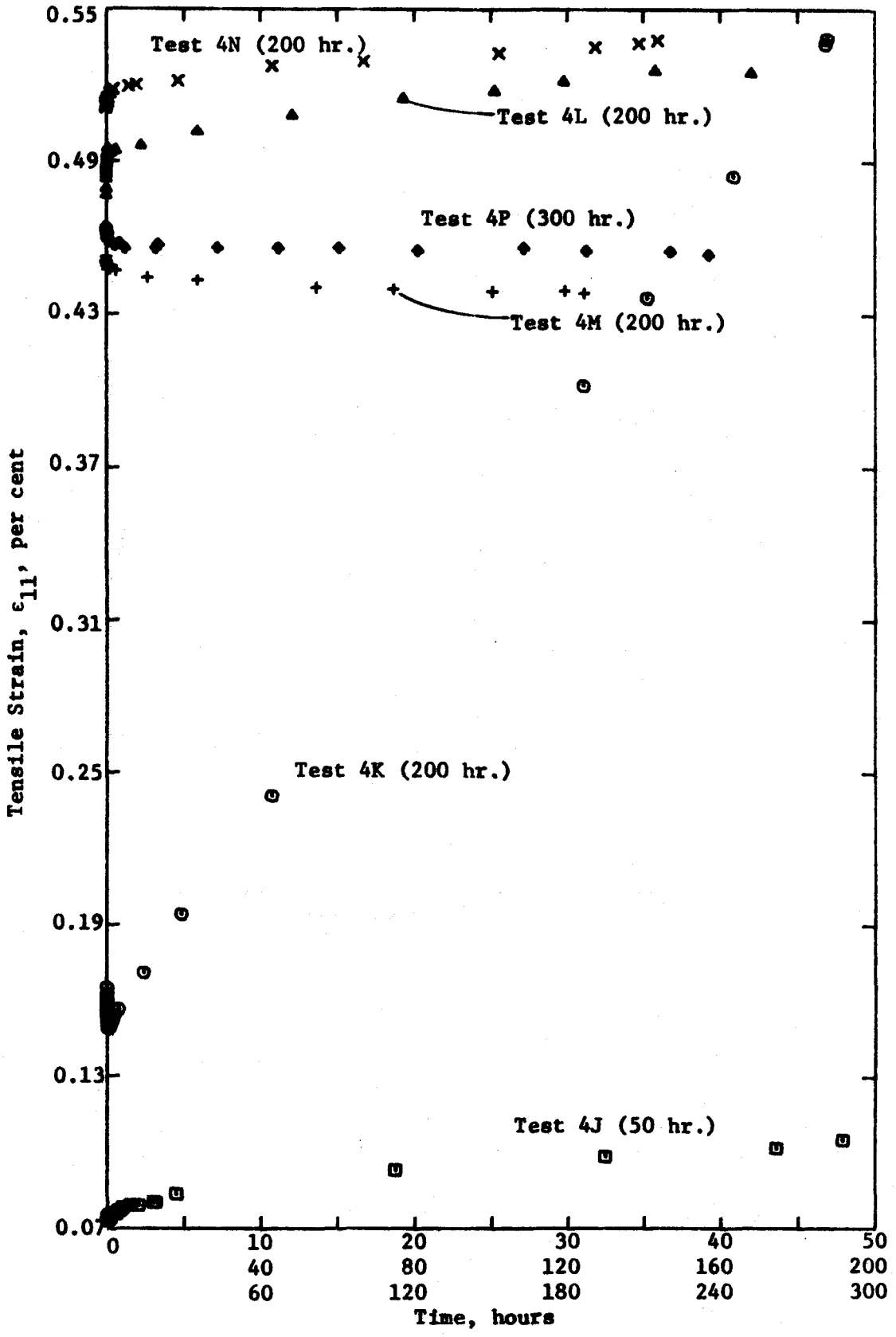


Fig. 4a. Supplementary Experiments for Test No. 4. (See Table VI.)

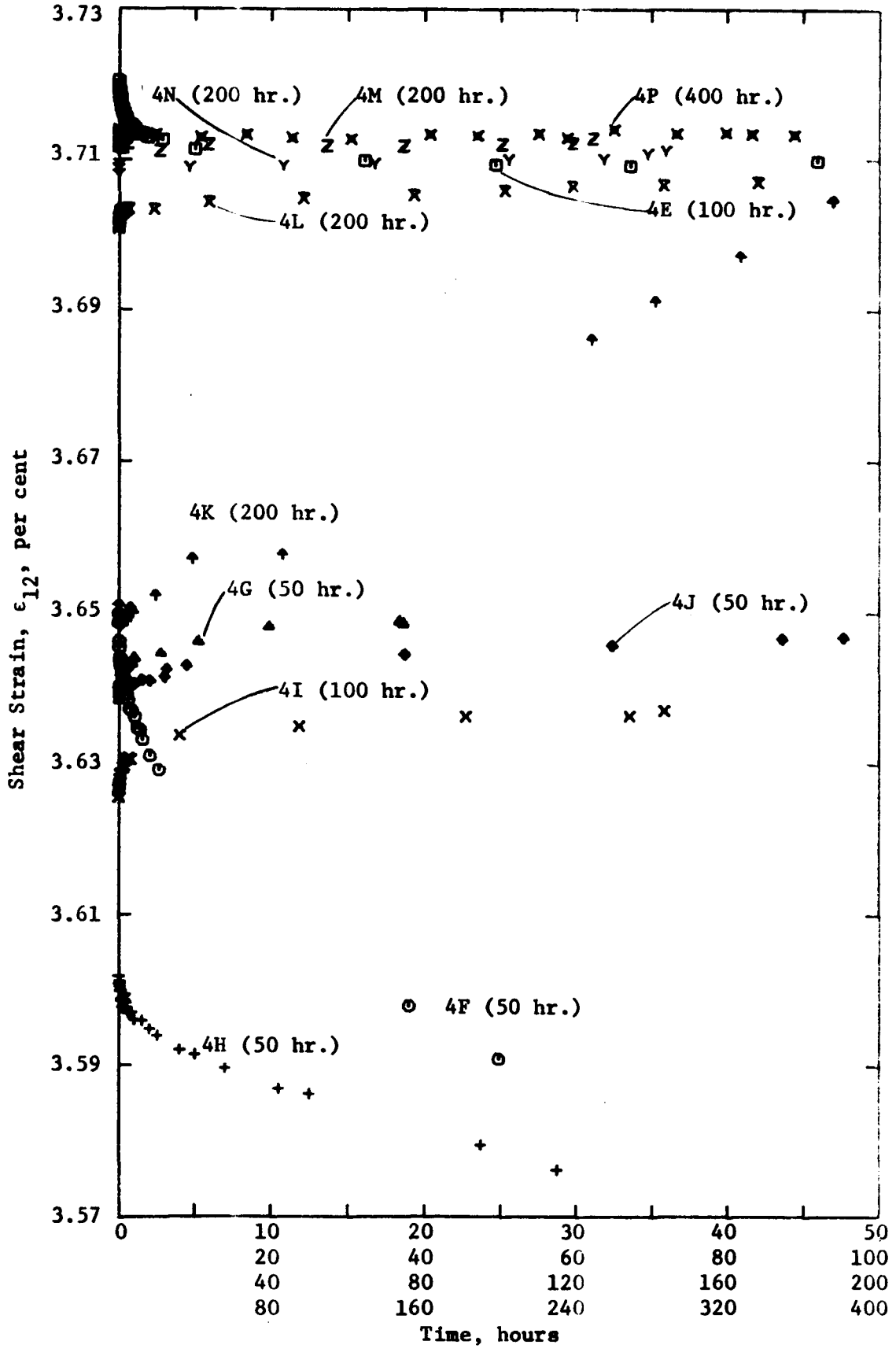


Fig. 4b. Supplementary Experiments for Test No. 4, continued. (See Table VI.)

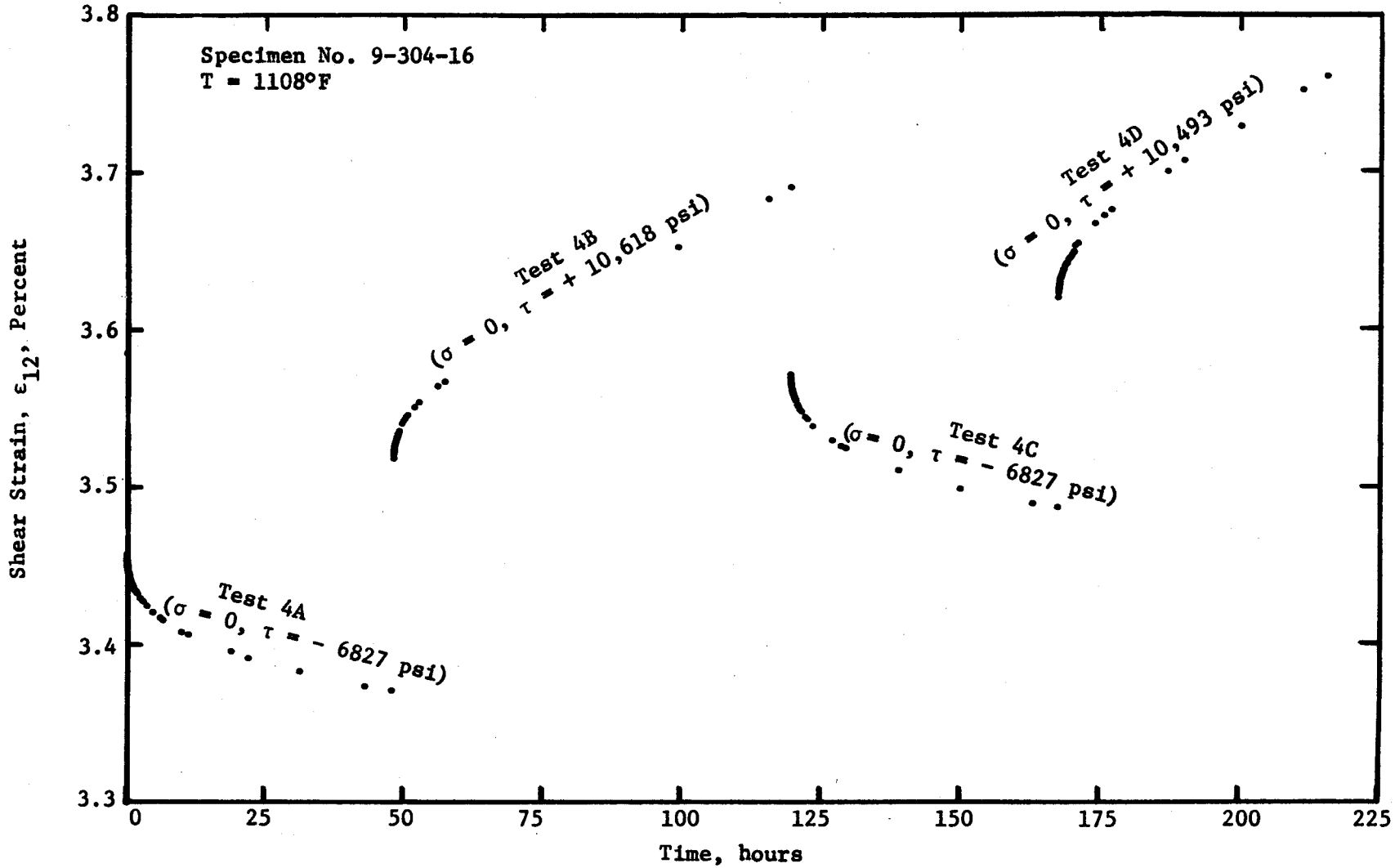


Fig. 4c. Stress Reversals Following Creep of Test No. 4 at $\tau$ = 10,493 for 1009.25 hr. (See Table VI.)

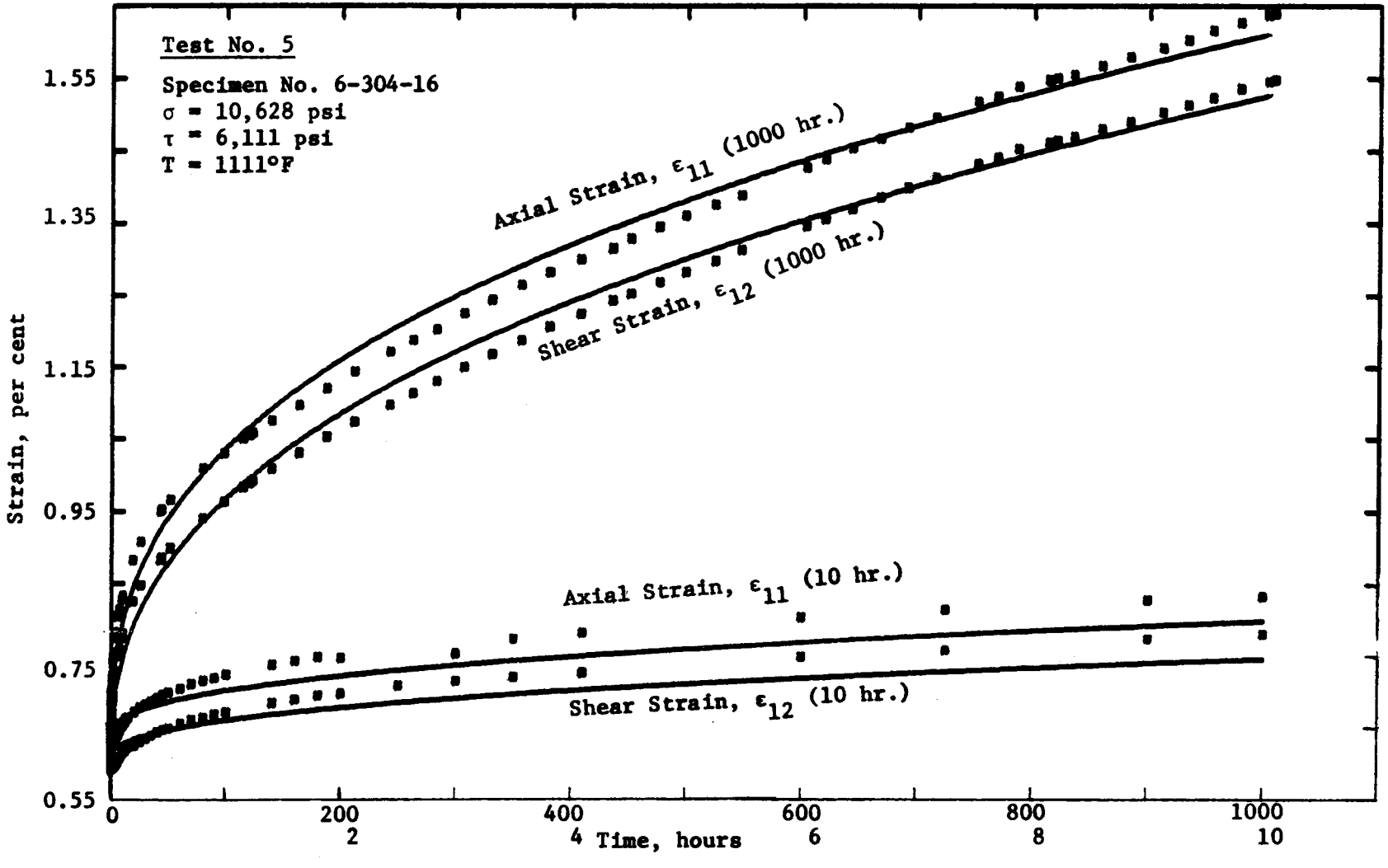


Fig. 5. Total Strain vs. Time during Constant Load Creep.

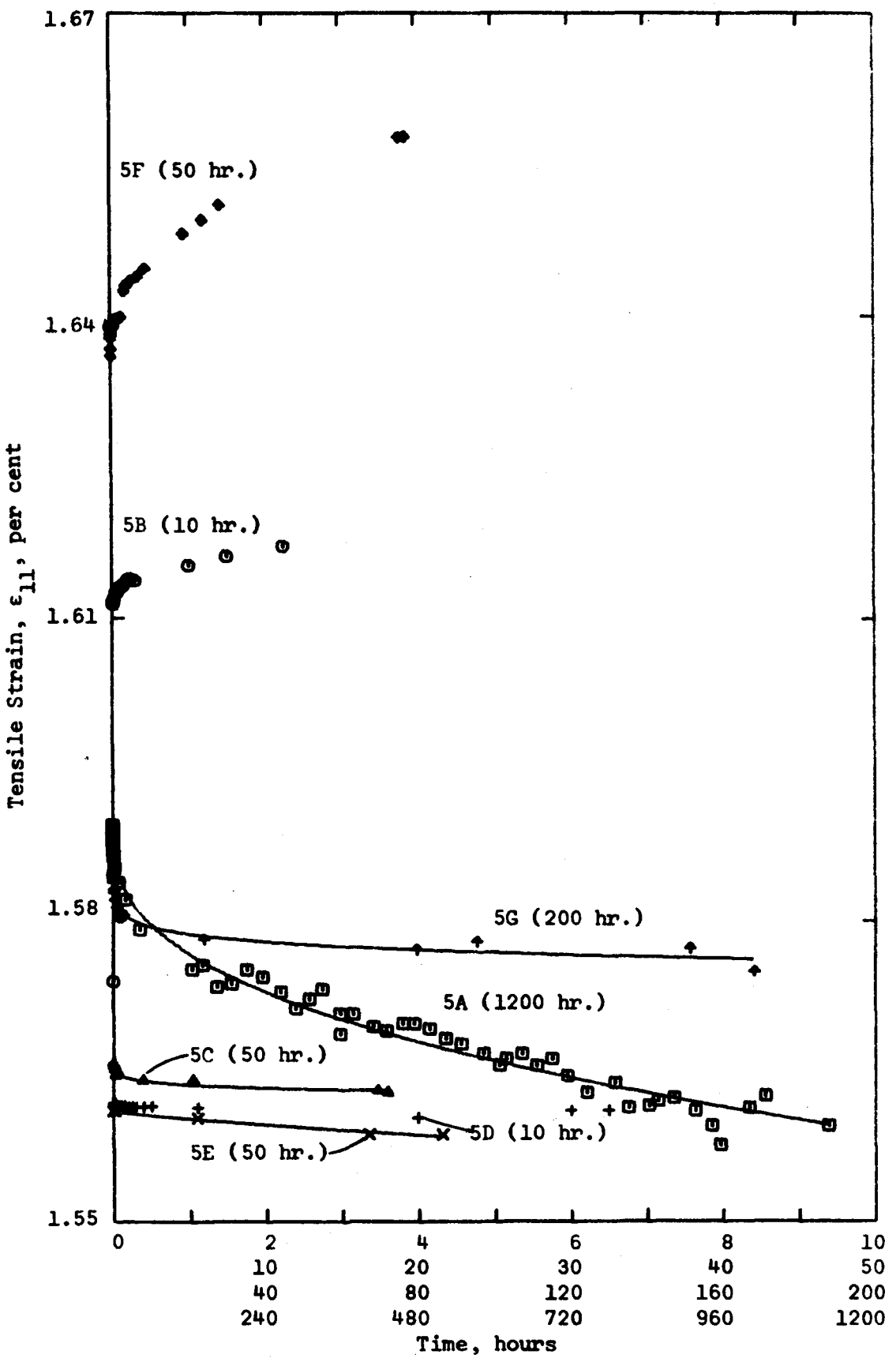


Fig. 5a. Supplementary Experiments for Test No. 5. (See Table VII.)

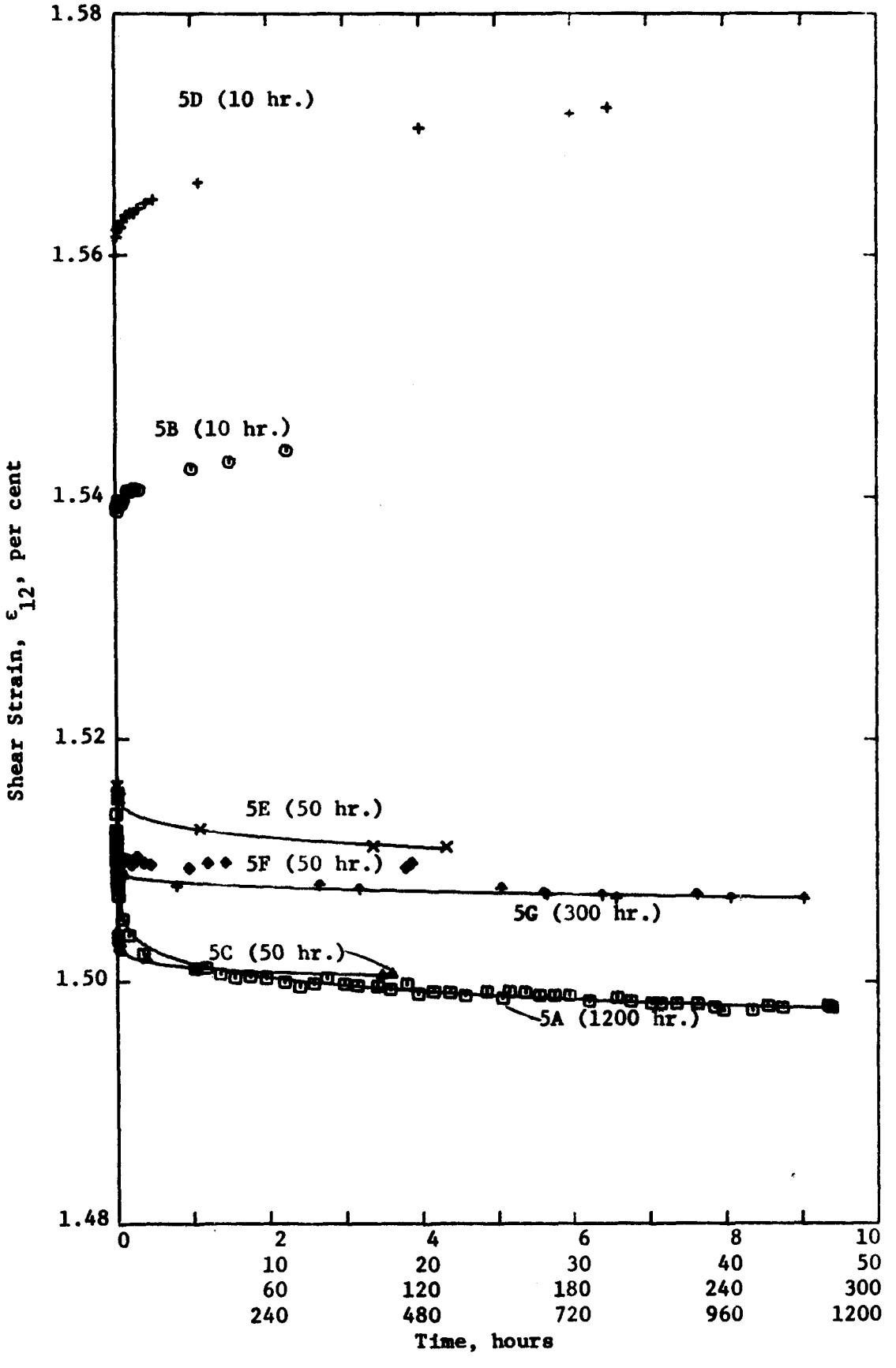


Fig. 5b. Supplementary Experiments for Test No. 5, continued. (See Table VII.)

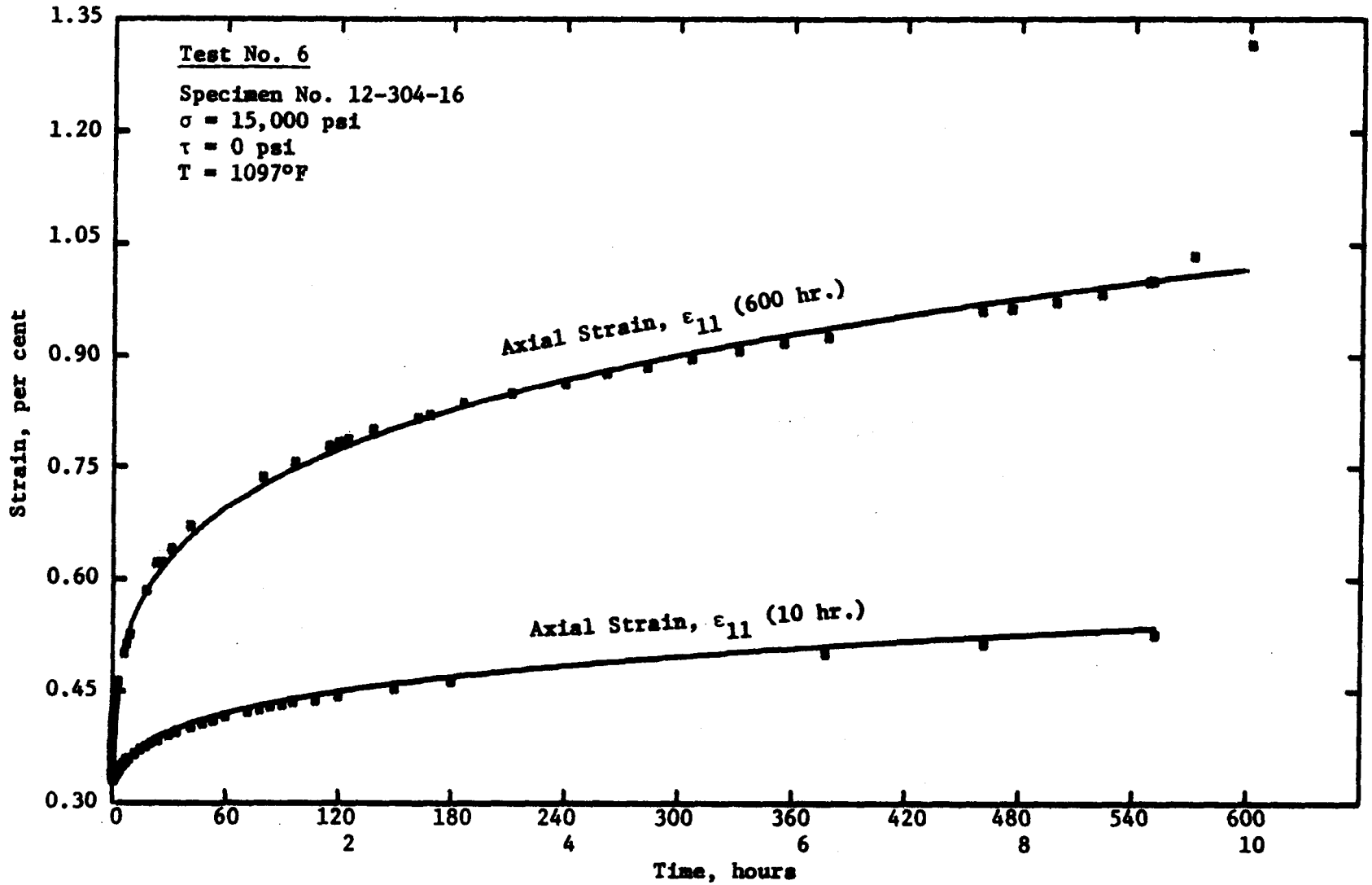


Fig. 6. Total Strain vs. Time during Constant Load Creep.

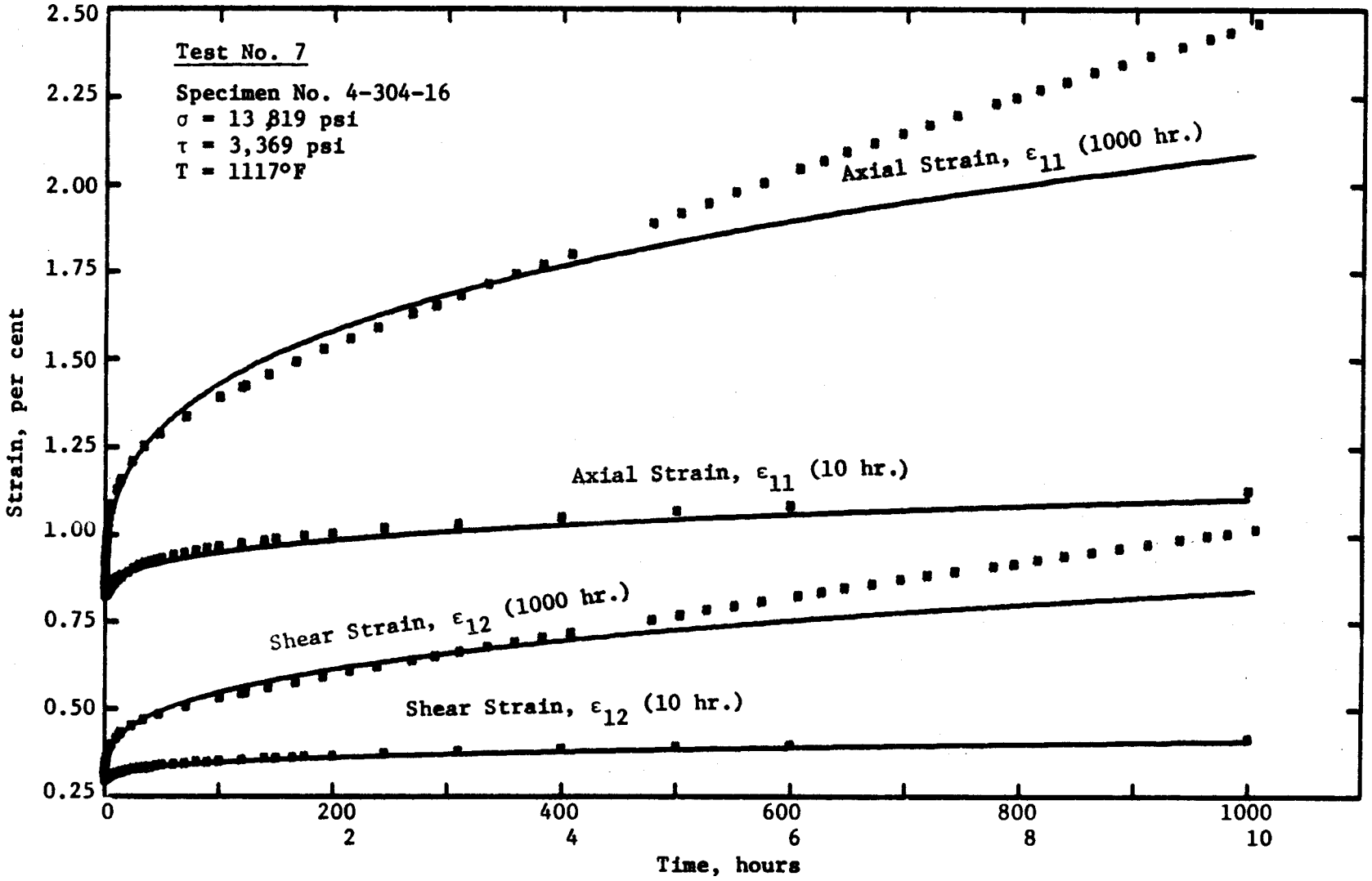


Fig. 7. Total Strain vs. Time during Constant Load Creep.

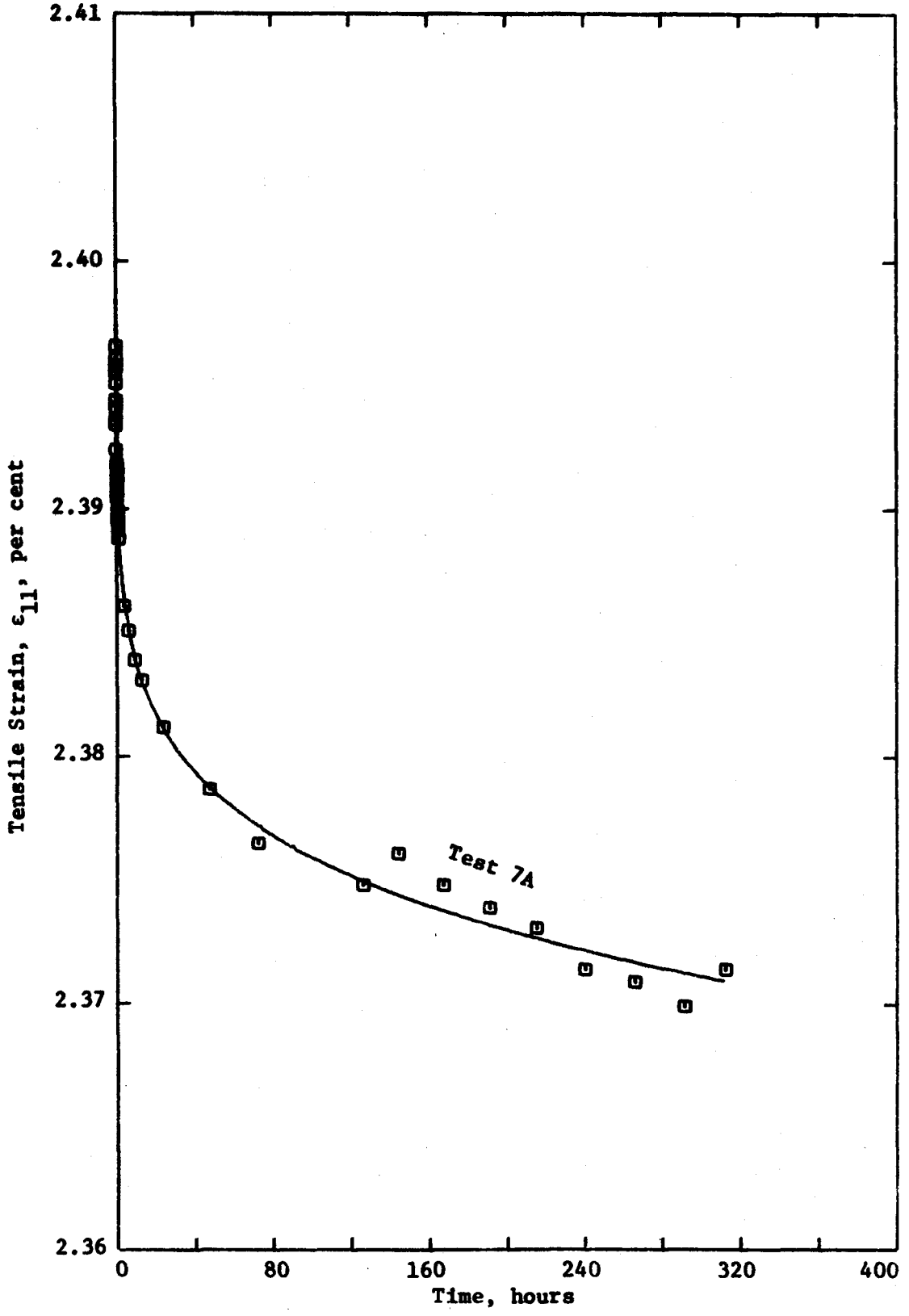


Fig. 7a. Recovery in Test No. 7.

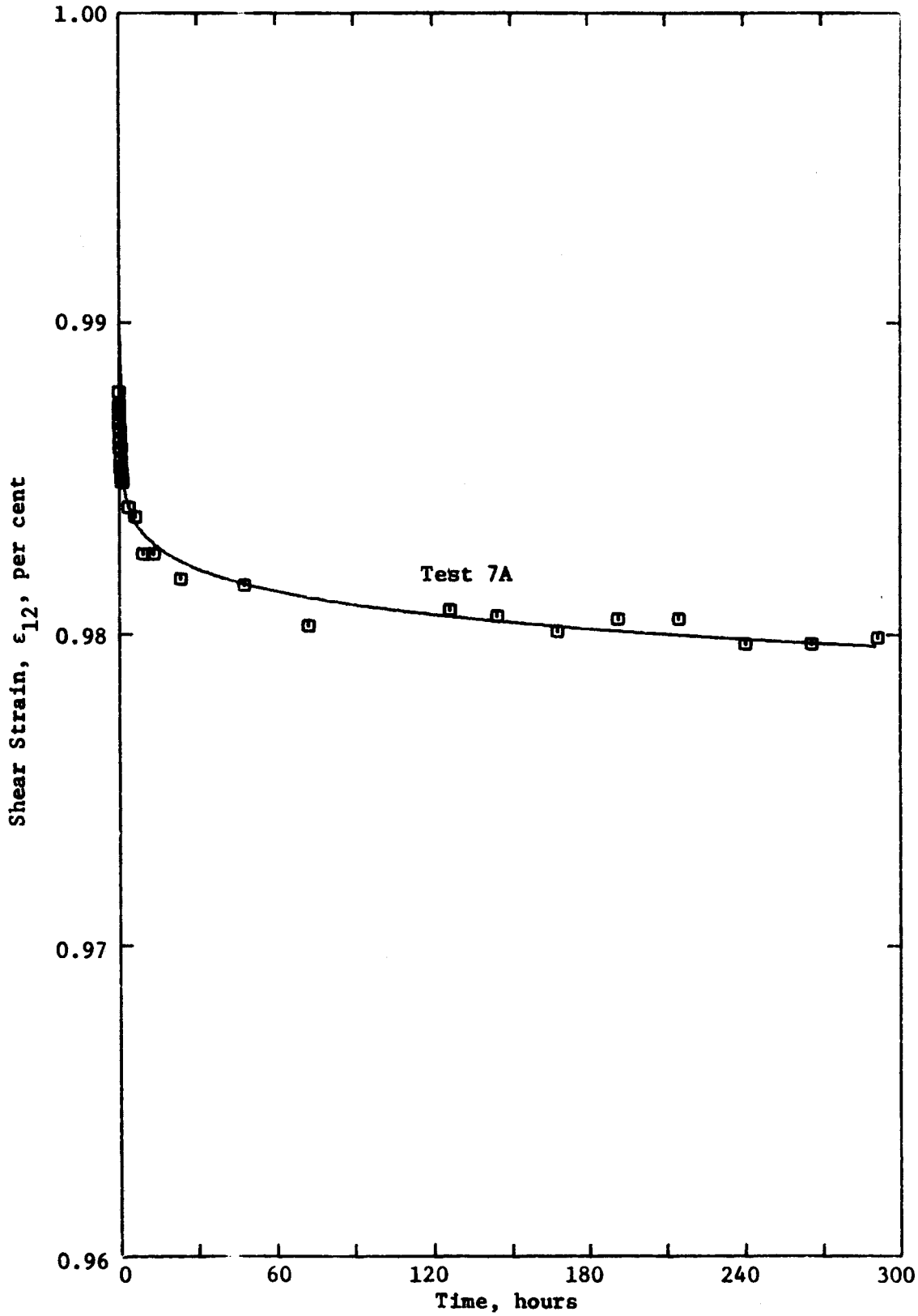


Fig. 7b. Recovery in Test No. 7, continued.

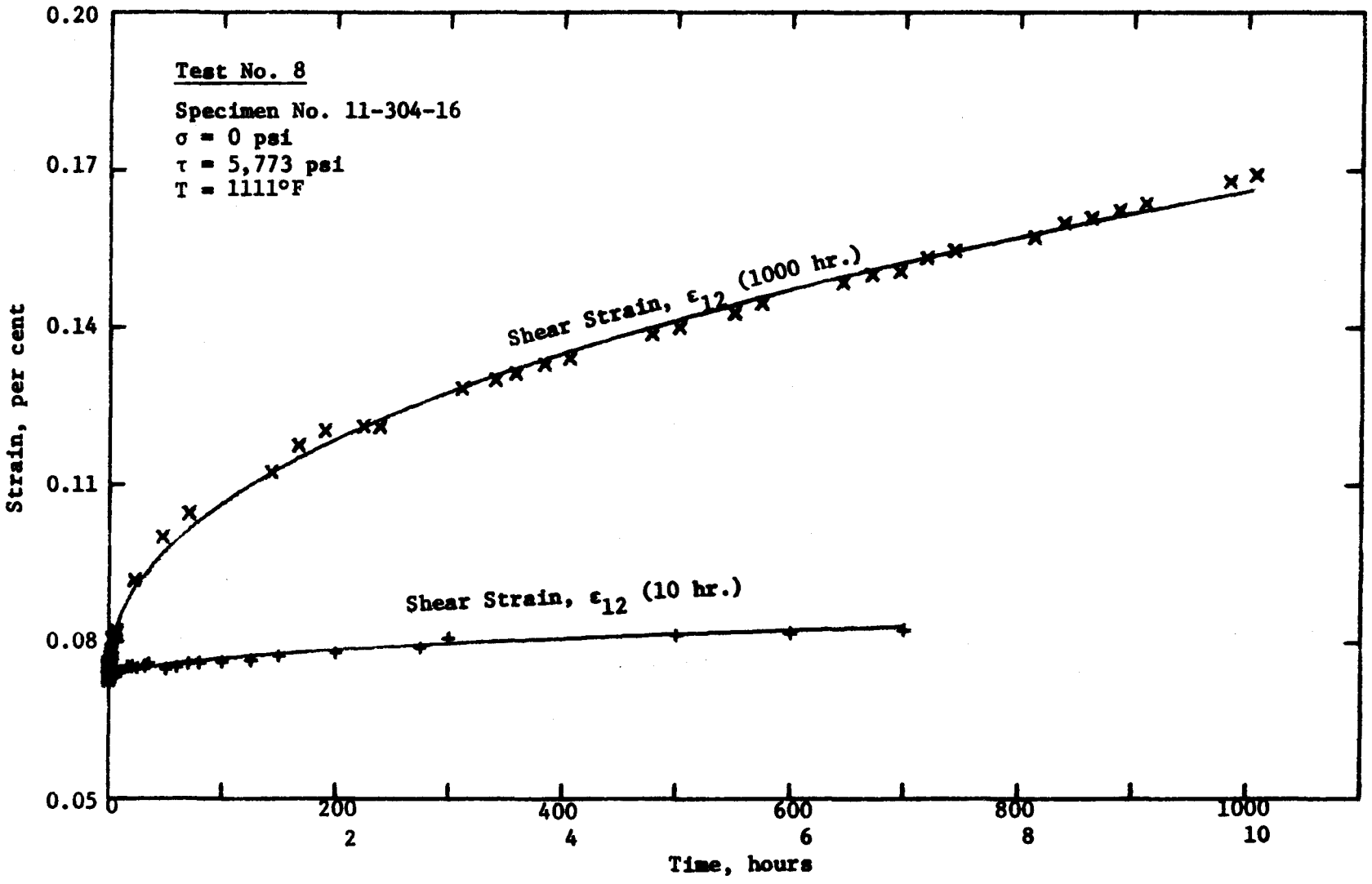


Fig. 8. Total Strain vs. Time during Constant Load Creep.

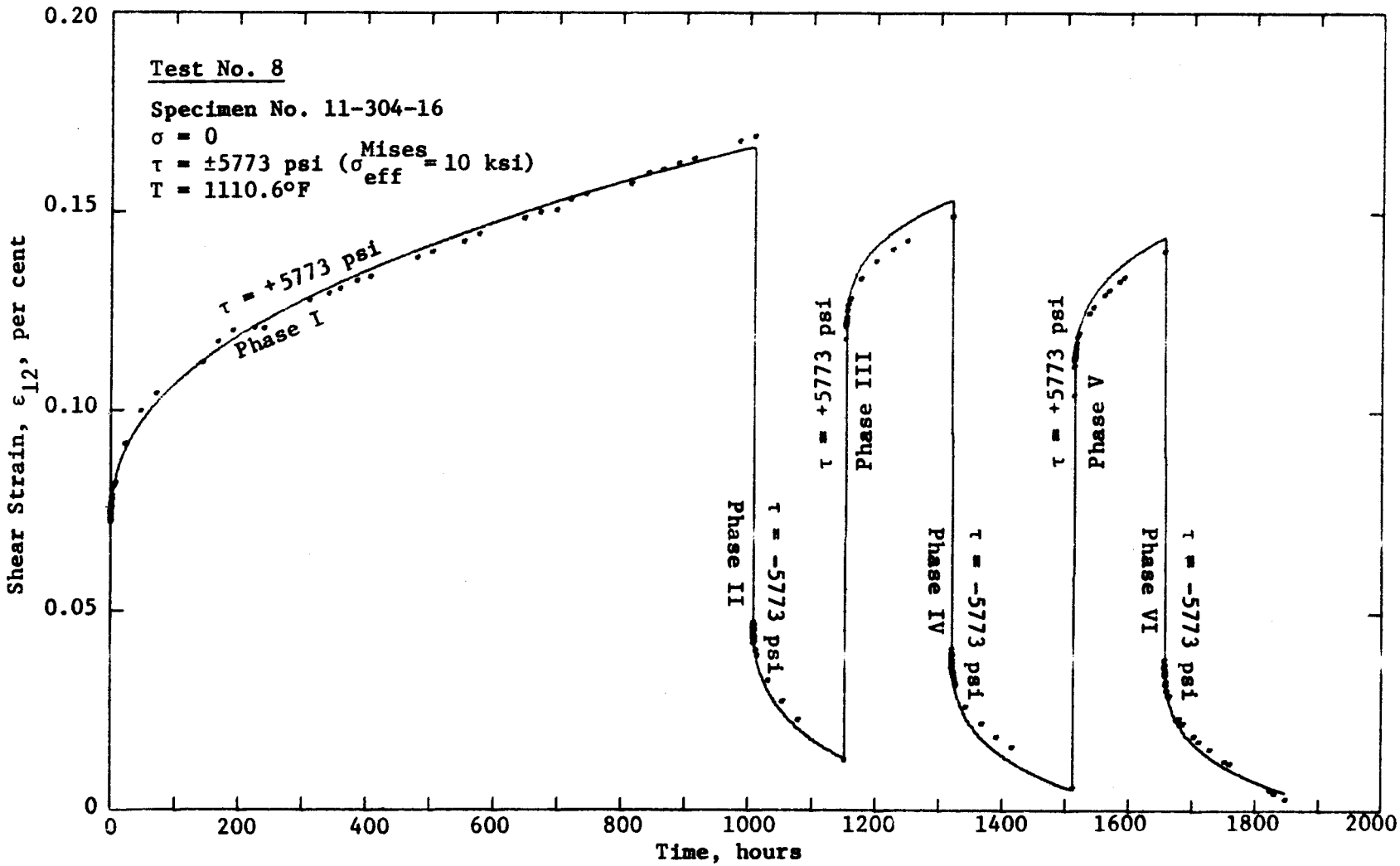


Fig. 8a. Stress Reversals after Long-Time Creep. Predictions based in part on a modified superposition principle. (See Table VIII.)

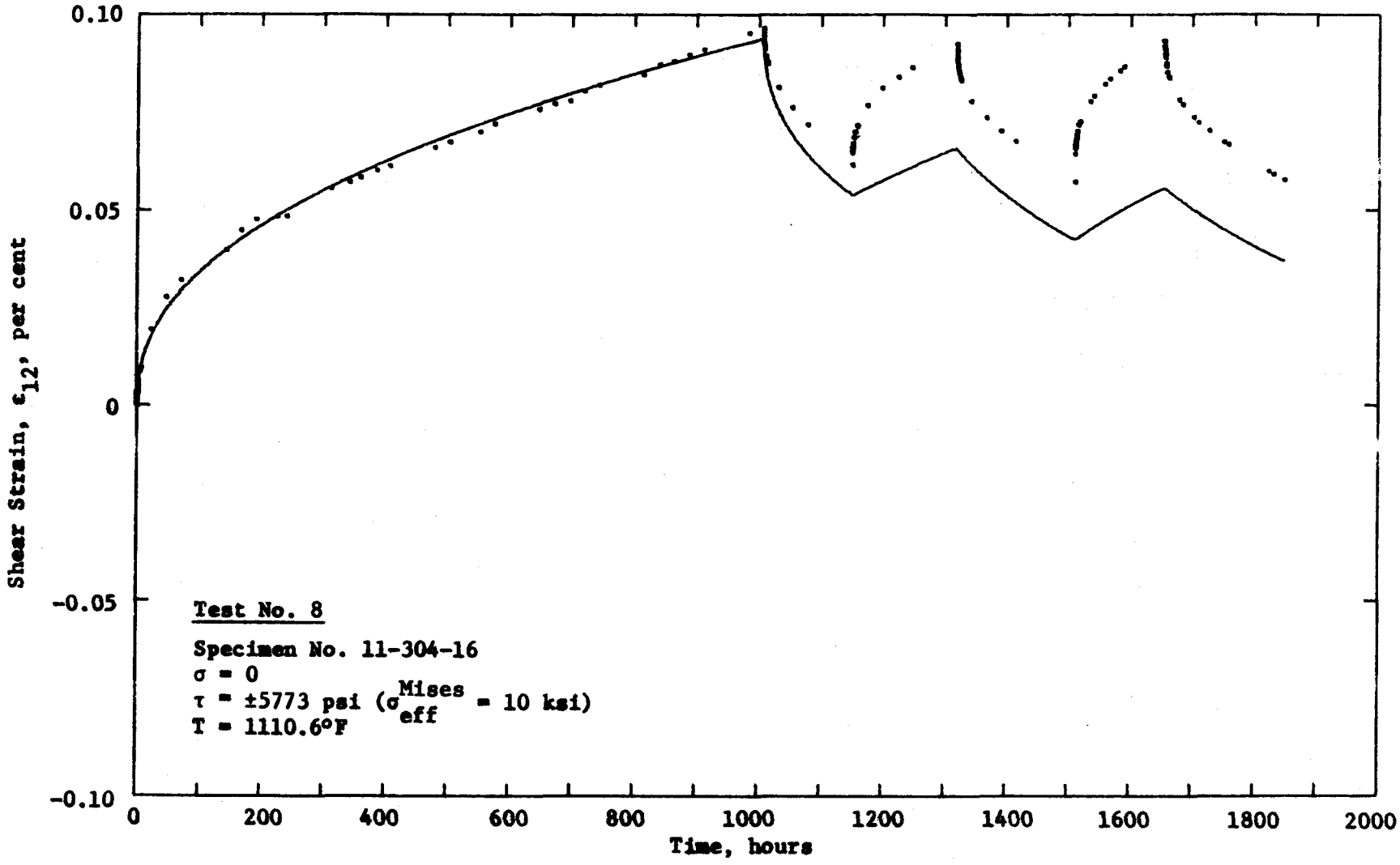


Fig. 8b. Creep under Stress Reversal as Predicted by Assuming Strain Hardening. (See Table VIII.)

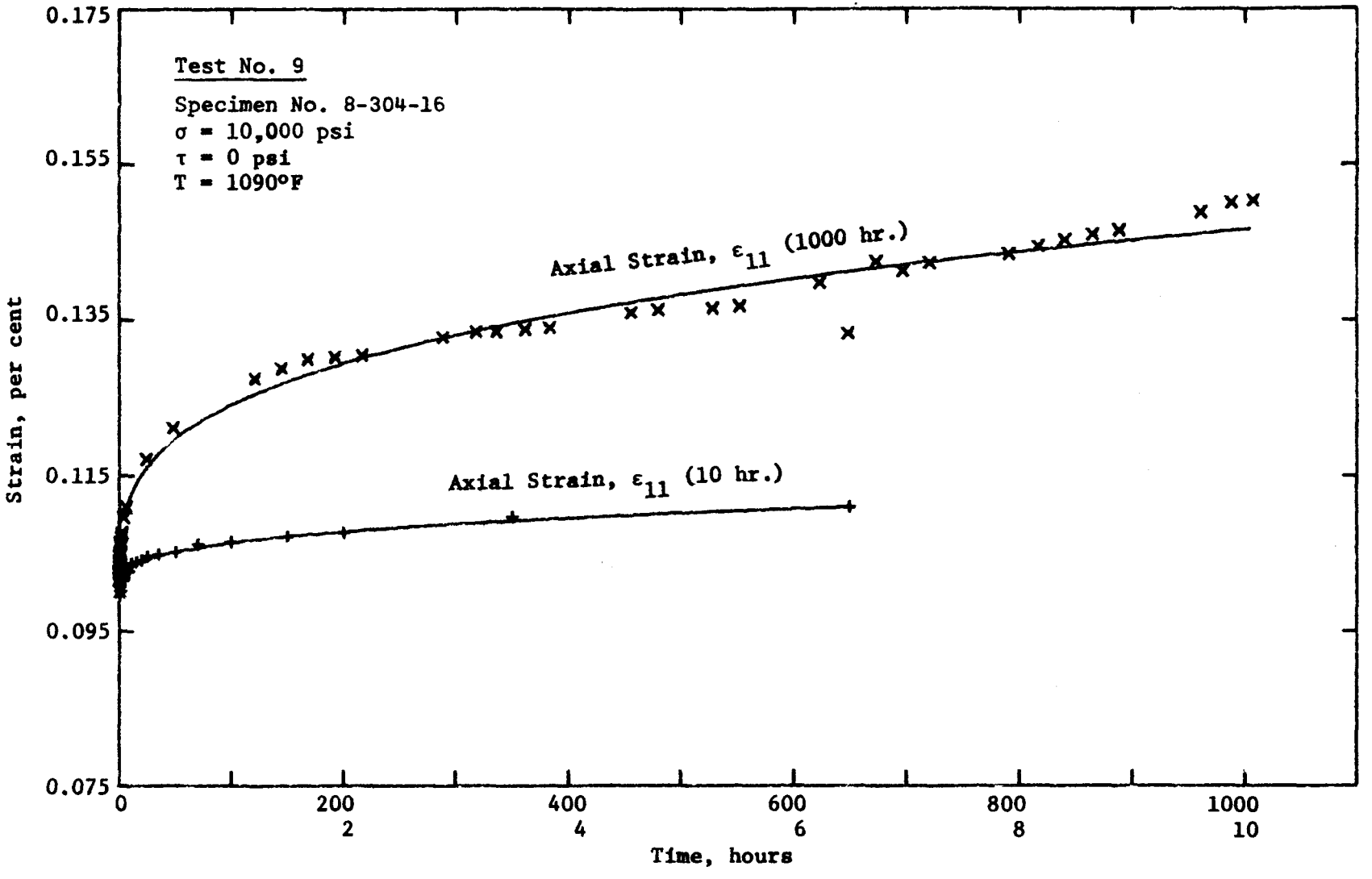


Fig. 9. Total Strain vs. Time during Constant Load Creep.

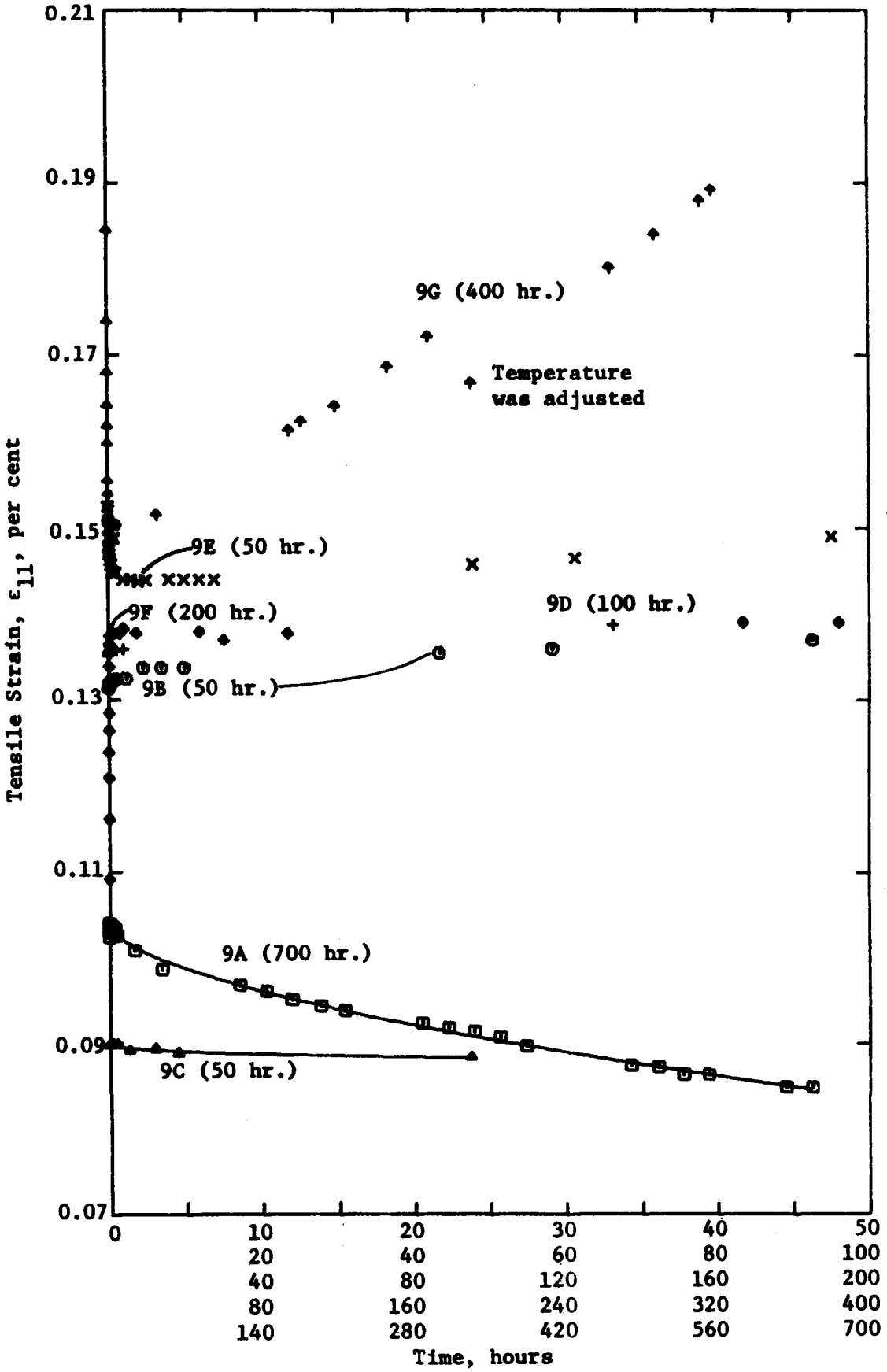


Fig. 9a. Supplementary Experiments in Test No. 9.
(See Table IX.)

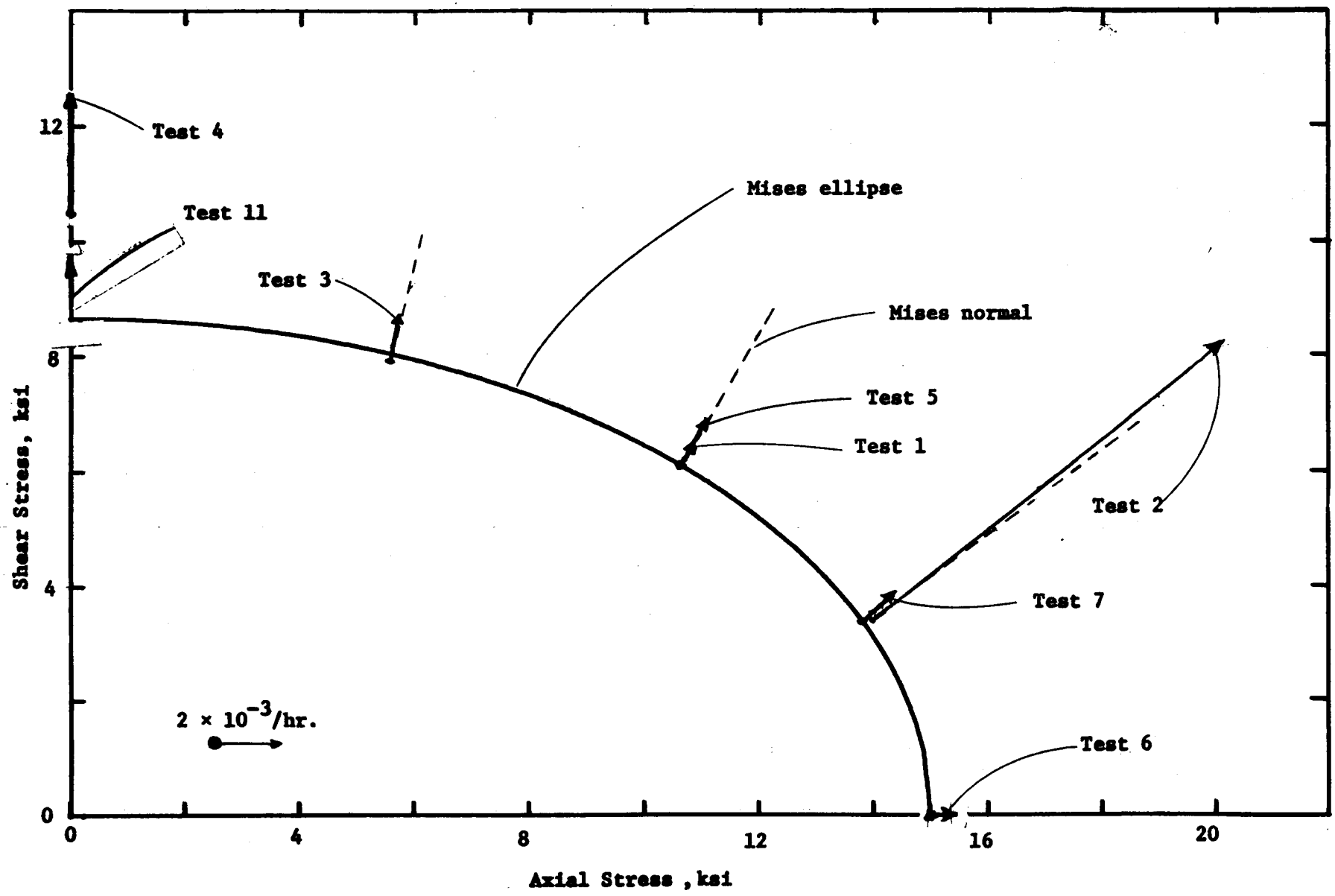


Fig. 10. Strain Rate Vectors of S.S. 304 at 120 hrs. and 1100°F, approximately.

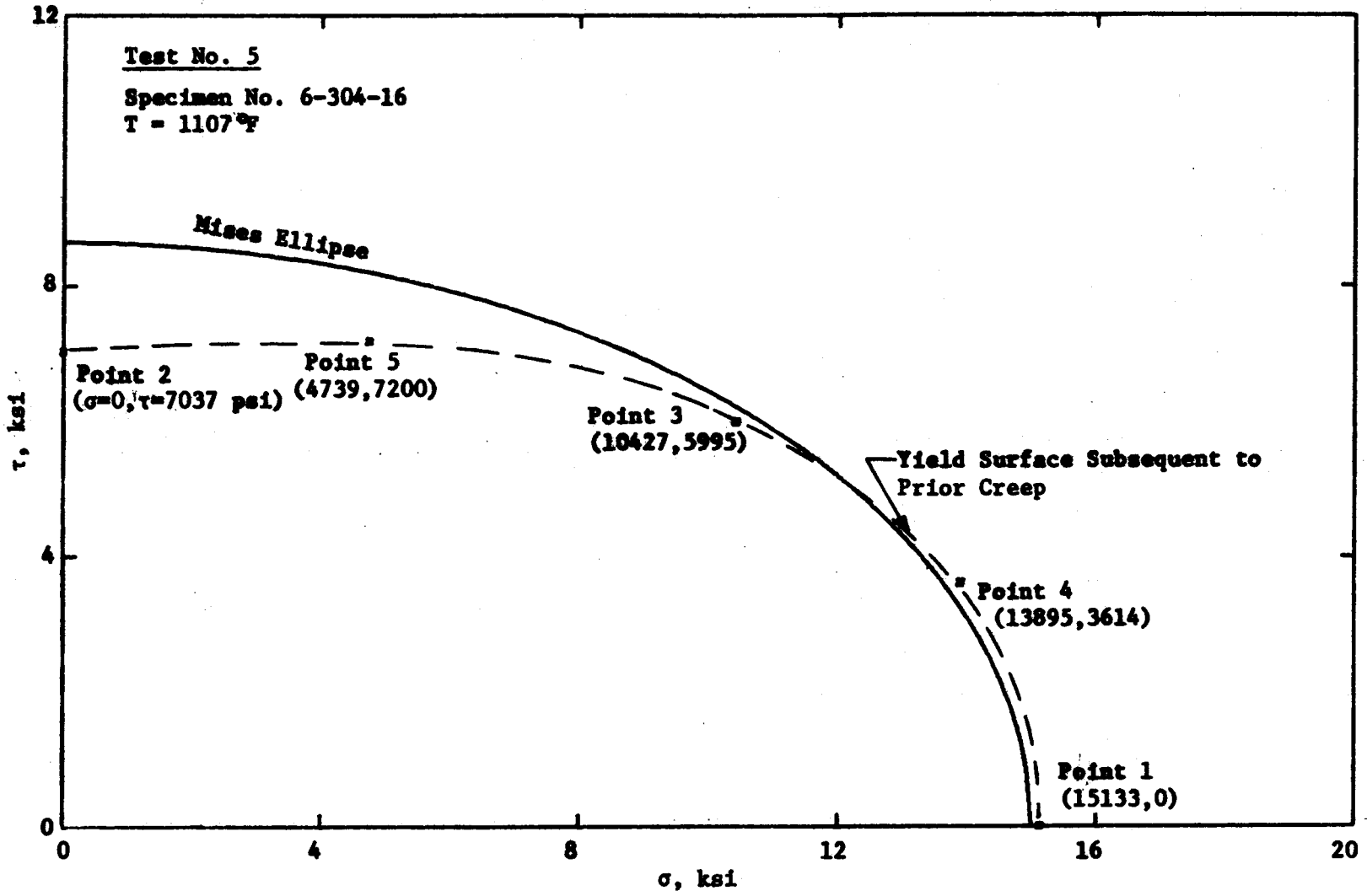


Fig. 11. Yield Surface for Specimen No. 6 Subsequent to Test No. 5G. (See Table VII.)

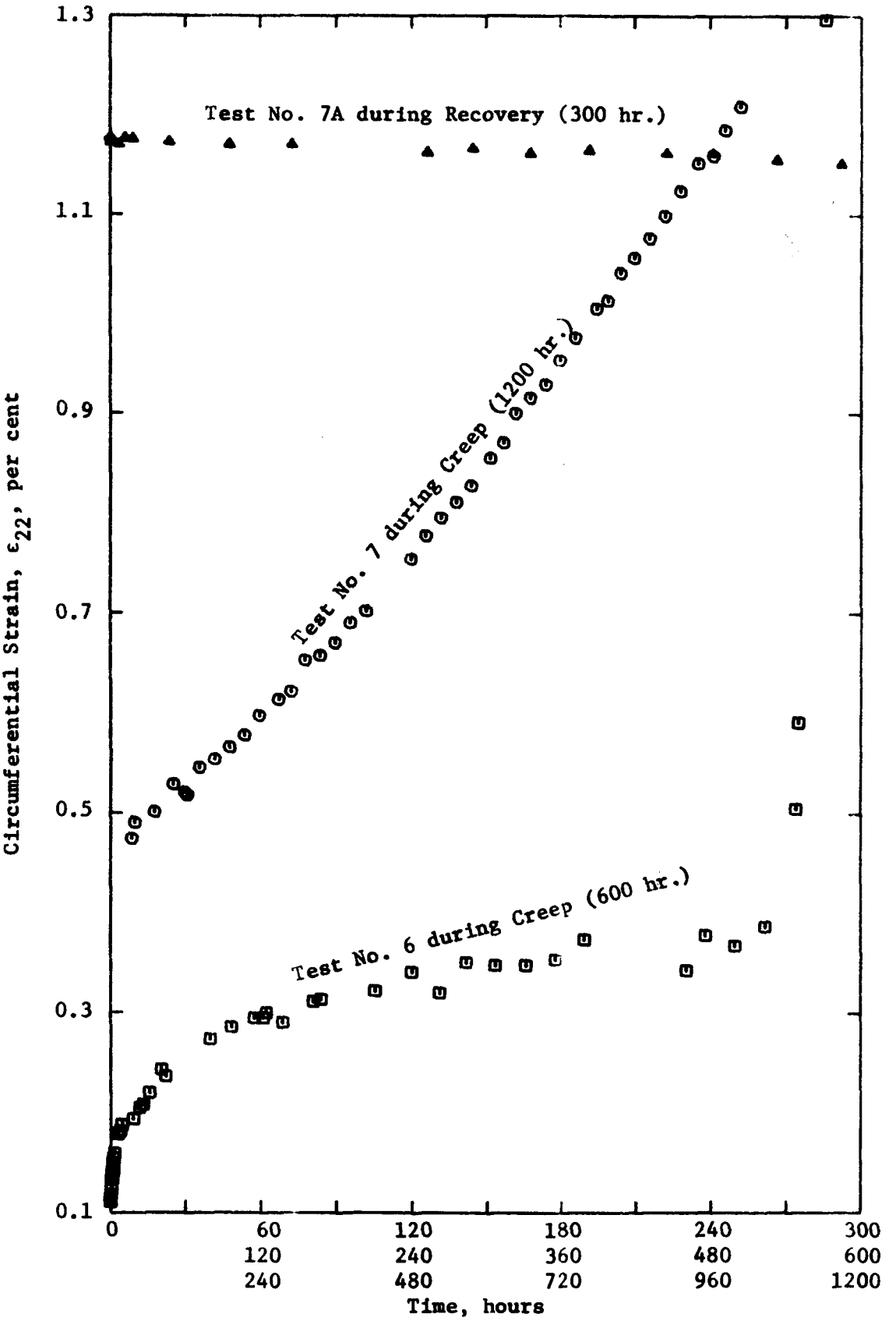


Fig. 12. Circumferential Strains in Tests 6 and 7. Strains shown in the figure are negative. (See Fig. 6 and 7.)